

# Geometry Eigenvalues and Scalar Product from Recoupling Theory in Loop Quantum Gravity

Roberto De Pietri\*

*Dipartimento Di Fisica, Università di Parma and  
I.N.F.N. Sezione di Milano, Gruppo Collegato di Parma,  
I-43100 Parma (PR), Italy*

Carlo Rovelli†

*Department of Physics and Astronomy,  
University of Pittsburgh, Pittsburgh Pa 15260, Usa  
(July 16, 2018)*

We summarize the basics of the loop representation of quantum gravity and describe the main aspects of the formalism, including its latest developments, in a reorganized and consistent form. Recoupling theory, in its graphical tangle-theoretic Temperley-Lieb formulation, provides a powerful calculation tool in this context. We describe its application to the loop representation in detail. Using recoupling theory, we derive general expressions for the spectrum of the quantum area and the quantum volume operators. We compute several volume eigenvalues explicitly. We introduce a scalar product with respect to which area and volume are symmetric operators, and (the trivalent expansions of) the spin network states are orthonormal.

04.60.-m, 02.70.-c, 04.60.Ds, 03.70.+k

## I. INTRODUCTION

We start with a citation from R. Penrose [1]: “My own view is that ultimately physical laws should find their most natural expression in terms of essentially combinatorial principles, that is to say, in terms of finite processes such as counting or other basically simple manipulation procedures. Thus, in accordance with such a view, some form of discrete or combinatorial space time should emerge.” The loop approach to quantum general relativity [2,3] seems to be leading precisely to a realization of such a vision of a combinatorial space-time, deriving it solely from a strict application of conventional quantum ideas to standard general relativity.<sup>1</sup>

A number of recent advances in this direction have strengthened this hope: a simplification of the formalism due to the introduction of the spin network basis [10–12]; the result that area [13] and volume operators [14,15] have discrete eigenvalues; the idea that in the presence of matter these eigenvalues might be taken as physical predictions on quantum geometry [16]; a novel approach that, among other results, re-derives loop-representation results from a general quantization program, and completes them using rigorous  $C^*$  algebraic and measure theoretical techniques [9,17,18]; a Hamiltonian generating clock time evolution [19] and a tentative perturbation scheme for computing diffeomorphism invariant transition amplitudes [20]; the extension of the theory to fermions [21] and to the electromagnetic field [22]. This rapid development has produced a certain amount of confusion in the notation and the basics of the theory. A first aim of this paper is to bring some order in the loop representation formalism, by presenting the basics formulas, notations and results in a consistent and self-contained form. This allows us to insert a novel sign factor into the very definition of the loop representation, short-cutting sign complications of the previous formulation. In a sense, we bring to full maturity the insights of reference [10].

With the new sign factor, loop states of the loop representation satisfy the axioms of Penrose’s “binor calculus” [23], or, equivalently, the axioms of the tangle-theoretic formulation of recoupling theory [24] for the special “classical” value  $A = -1$  of the deformation parameter. This fact brings a powerful set of computational techniques at the service of quantum gravity. We describe here in detail how this calculus can be used. Calculations in loop quantum gravity were first performed using the grasping operation on single loops [3]. It was then realized, mainly in [18],

---

\*E-mail address: depietri@vaxpr.pr.infn.it

†E-mail address: roveli@pitt.edu

<sup>1</sup>For an overview of current ideas on quantum geometry, see [4], [5] and [6]; for a recent overview of canonical gravity, see [7]; for detailed introductions to loop quantum gravity, see [8] and [9].

that such combinatorial techniques admitted a group theoretical interpretation ( $su(2)$  representation theory admits a fully combinatorial description). Recoupling theory is a further –and far more powerful– level of sophistication for the same calculus.

The idea that recoupling theory plays a role in loop quantum gravity has been advocated by Reisenberger [25] and by Smolin. Motivated by certain physical and mathematical considerations, Borissov, Major and Smolin [26,27] have considered deformations of the standard loop representation theory. Recoupling theory with general values of the deformation parameter  $A$  plays a key role in the definition of these deformations. What we do here is very different in spirit: we remain within the framework of the standard loop-representation quantum GR, and use recoupling theory merely as a computational tool.

Using recoupling theory, we derive general formulas for area and volume in quantum gravity. The spectrum of the area agrees with previously published results [14]. The derivation presented here is simpler and more elegant than the one in Ref. [14]. The first of our main new results is a general formula for the volume. We present it here expressed in terms of  $su(2)$  6-j symbols (and related quantities). We confirm the fact that trivalent vertices have zero volume, first pointed out by Loll [15]. We explicitly compute many eigenstates for four- and five-valent vertices. Loll has computed a few of these eigenvalues in [28] using a different technique. We find agreement with the numbers published by Loll (see also [27]). We show that the absolute value and the square root that appear in the definition of the volume operator are well defined. Indeed, we show that the arguments of the absolute value are finite dimensional matrices diagonalizable and with real eigenvalues; and that the arguments of the square root are finite dimensional matrices diagonalizable and with real non-negative eigenvalues. We show in general that the eigenvalues of the volume are real and non-negative.

Finally, the technique introduced allows us to define a scalar product in the loop representation, by requiring that area and volume be symmetric, and that spin network states be orthogonal to each other – whatever the trivalent decomposition of high valence vertices we use. This is our second main new result.

The structure of this paper is the following. In Sec. II, we review the basics of the Ashtekar formulation of general relativity and we define the loop variables (in the new form that leads directly to recoupling theory). In Sec. III, we derive the basic equations of the loop representation. In Sec. IV we discuss the role of recoupling theory. In Sec. V we define the spin network basis. In Sec. VI, we discuss the area operator, and in Sec. VII the volume operator. In Sec. VIII we define the scalar product. Sec. IX contains our conclusions.

## II. LOOP VARIABLES IN CLASSICAL GR

We begin by reviewing the canonical formulation of general relativity in the Ashtekar formalism [29]. This is given as follows. We fix a three-dimensional manifold  $M$  and consider two (smooth) complex  $SO(3)$  fields  $A_a^i(x)$  and  $\tilde{E}_i^a(x)$  on  $M$ . We use  $a, b, \dots = 1, 2, 3$  for (abstract) spatial indices and  $i, j, \dots = 1, 2, 3$  for internal  $SO(3)$  indices. We indicate coordinates on  $M$  with  $\mathbf{x}$ . The relation between these fields and conventional metric gravitational variables is as follows:  $A_a^i(x)$  is the projection of the self-dual part of the gravitational spin-connection on a constant time surface;  $\tilde{E}_i^a(x)$  is the (densitized) inverse triad, related to the three-dimensional metric  $g_{ab}(x)$  of the constant-time surface by

$$g_{ab} = \tilde{E}_i^a \tilde{E}_i^b, \quad (2.1)$$

where  $g$  is the determinant of  $g_{ab}$ . It is useful for what follows to consider the dimensional character of the field with care. We set the dimension of the fields as follow:

$$\begin{aligned} [g_{ab}] &= L^2, & [\tilde{E}_i^a] &= L^2, \\ [A_a^i] &= \text{dimensionless}. \end{aligned} \quad (2.2)$$

The popular choice of taking the metric dimensionless is not very sensible in GR. It forces coordinates to have dimensions of a length; but the freedom of arbitrary transformations on the coordinates is hardly compatible with dimensional coordinates. Coordinates, for instance, can be angles, and assigning angles dimension of a length makes no sense. The Einstein action can be rewritten (see for example [8]) as

$$S = \frac{1}{G} \int d^4x \sqrt{g} R = \frac{1}{G} \int dx^0 \int d^3x \left[ -i \dot{A}_a^i \tilde{E}_i^a + i \dot{A}_0^i \tilde{C}_i + i N^a \tilde{C}_a + \tilde{N} \tilde{W} \right], \quad (2.3)$$

where we have set

$$G = \frac{16\pi G_{\text{Newton}}}{c^3} \quad (2.4)$$

$G_{\text{Newton}}$  being Newton's gravitational constant, and  $\tilde{C}_i$ ,  $\tilde{C}_a$ ,  $\tilde{W}$  the diffeomorphism, Gauss and Hamiltonian constraints. It follows that the momentum canonically conjugate to  $A_a^i$  is

$$p_i^a(x) = \frac{\delta S}{\delta \dot{A}_a^i(x)} = -\frac{i}{G} \tilde{E}_i^a. \quad (2.5)$$

and therefore the fundamental Poisson bracket of the Hamiltonian theory is

$$\{A_a^i(x), \tilde{E}_j^b(y)\} = iG \delta_a^b \delta_j^i \delta^3(x, y) \quad (2.6)$$

The spinorial version of the Ashtekar variables is given in terms of the Pauli matrices  $\sigma_i, i = 1, 2, 3$ , or the  $su(2)$  generators  $\tau_i = -\frac{i}{2} \sigma_i$ , by

$$\tilde{E}^a(x) = -i \tilde{E}_i^a(x) \sigma_i = 2\tilde{E}_i^a(x) \tau_i \quad (2.7)$$

$$A_a(x) = -\frac{i}{2} A_a^i(x) \sigma_i = A_a^i(x) \tau_i. \quad (2.8)$$

$A_a(x)$  and  $\tilde{E}^a(x)$  are  $2 \times 2$  complex matrices. We use upper case indices  $A, B, \dots = 1, 2$  for the spinor space on which the Pauli matrices act. Thus, the components of the gravitational fields are  $A_{aA}{}^B(x)$  and  $\tilde{E}^a{}_A{}^B(x)$ .

In order to construct the loop variables, we start from some definitions.

**Segment.** A segment  $\gamma$  is a continuous and piecewise smooth map from the closed interval  $[0, 1]$  into  $M$ . We write:  
 $\gamma : s \mapsto \gamma^a(s)$ .

**Loop.** A loop  $\alpha$  is a segment such that  $\alpha^a(0) = \alpha^a(1)$ . Equivalently, it is a continuous, piecewise smooth, map from the circle  $S_1$  into  $M^3$ .

**Free Loop Algebra.** We consider (formal) linear combinations  $\Phi$  of (formal) products of loops, as in:

$$\Phi = c_0 + \sum_i c_i [\alpha_i] + \sum_{jk} c_{jk} [\alpha_j][\alpha_k] + \dots, \quad (2.9)$$

where the  $c$ 's are arbitrary complex number and the  $\alpha$ 's are loops; we denote the space of such objects as the Free Loop Algebra  $\mathcal{A}^f[\mathcal{L}]$ . (See also [9])

**Multiloop.** We denote the monomials in  $\mathcal{A}^f[\mathcal{L}]$ , namely the elements of the form  $\Phi = [\alpha_1] \dots [\alpha_n]$  as multiloops. We indicate multiloops by a Greek letter, in the same manner as (single) loops:  $[\alpha] = [\alpha_1] \dots [\alpha_n]$ .

Given a segment  $\gamma$ , we consider the parallel propagator of  $i$  times  $A_a$  along  $\gamma$ . This is defined by the equation

$$\frac{d}{d\tau} U_\gamma(\tau, \tau_0) + \frac{d\gamma^a(\tau)}{d\tau} i A_a(\gamma(\tau)) U_\gamma(\tau, \tau_0) = 0, \quad (2.10)$$

with the boundary condition  $U_\gamma(\tau_0, \tau_0)_A^B = \delta_A^B$ . The formal solution is

$$U_\gamma(\tau, \tau_0) = \mathcal{P} e^{-i \int_{\tau_0}^{\tau} d\tau \dot{\gamma}^a A_a(\gamma(\tau))}, \quad (2.11)$$

where  $\mathcal{P}$  indicates the path ordering of the exponential. We also write—in somewhat imprecise notation— $U_\gamma = U_\gamma(0, 1)$  and  $U_\gamma(s_2, s_1) = U_\gamma(\tau_2, \tau_1)$  if  $s_2 = \gamma(\tau_2)$  and  $s_1 = \gamma(\tau_1)$ .

Notice that we do not consider the parallel propagator of the Ashtekar connection, but the parallel propagator of  $i$  times the Ashtekar connection. With this choice, we are going to define a representation distinct from the one defined without the  $i$ ; in the sense that the state  $\langle \alpha |$  has a different physical meaning—different expectation value for the same physical operators—in the two cases. The choice we take here will later prove essential for the determination of the eigenstates of area and volume with real eigenvalues.

We can now define the fundamental loop variables. Given a loop  $\alpha$  and the points  $s_1, s_2, \dots, s_n \in \alpha$  we define:

$$\mathcal{T}[\alpha] = -\text{Tr}[U_\alpha], \quad (2.12)$$

$$\mathcal{T}^a[\alpha](s) = -\text{Tr}[U_\alpha(s, s) \tilde{E}^a(s)] \quad (2.13)$$

and, in general

$$\begin{aligned}\mathcal{T}^{a_1 a_2}[\alpha](s_1, s_2) &= -\text{Tr}[U_\alpha(s_1, s_2)\tilde{E}^{a_2}(s_2)U_\alpha(s_2, s_1)\tilde{E}^{a_1}(s_1)], \\ \mathcal{T}^{a_1 \dots a_N}[\alpha](s_1, \dots, s_N) &= -\text{Tr}[U_\alpha(s_1, s_N)\tilde{E}^{a_N}(s_N)U_\alpha(s_N, s_{N-1}) \dots U_\alpha(s_2, s_1)\tilde{E}^{a_1}(s_1)].\end{aligned}\quad (2.14)$$

The function  $\mathcal{T}[\alpha]$  defined in (2.12) for a single loop, can be defined over the whole free loop algebra  $\mathcal{A}^f[\mathcal{L}]$ : given the generic element  $\Phi \in \mathcal{A}^f[\mathcal{L}]$  in (2.9), we pose

$$\mathcal{T}[\Phi] = -2c_0 + \sum_i c_i \mathcal{T}[\alpha_i] + \sum_{ij} c_{ij} \mathcal{T}[\alpha_i] \mathcal{T}[\alpha_j] + \dots \quad (2.15)$$

The reason for the  $-2$  in the first term is the following. We may think of the first term of the sum as corresponding to the “point loop”, or a loop whose image is a point. For this loop, the exponent in (2.11) is zero, the holonomy is the identity (in  $sl(2, C)$ , namely in 2d) and  $\mathcal{T}$  is therefore  $-2$ .

Notice that there is a sign difference between the usual loops observables [2,3] (denoted  $T$ -variables) and these new loop observables, denoted  $\mathcal{T}$ -variables. This is a key technicality at the origin of the simplification of the formalism presented here. The new sign takes care immediately of the sign complications extensively discussed in reference [10]. The suggestion that those sign complications could be avoided by inserting a minus sign in front of the trace was considered by S. Major as well. Let us illustrate the consequences of having this sign. Consider an  $N$  component multiloop  $\alpha = \alpha_1 \alpha_2 \dots \alpha_N$ . We have:

$$\begin{aligned}\mathcal{T}[\alpha_1] \dots \mathcal{T}[\alpha_N] &= \mathcal{T}[\alpha_1] \dots \mathcal{T}[\alpha_1] \\ &= (-\text{Tr}[U_{\alpha_1}]) \dots (-\text{Tr}[U_{\alpha_N}]) \\ &= (-1)^N \text{Tr}[U_{\alpha_1}] \dots \text{Tr}[U_{\alpha_N}] \\ &= (-1)^N T[\{\alpha\}].\end{aligned}$$

This shows that the new sign choice implements in the formalism the sign factor for the number of loops that was recognized in [10] as the key to transform the spinor relation into a local relation. In fact, we have

$$\text{Tr}[U_\alpha] \text{Tr}[U_\beta] - \text{Tr}[U_\alpha U_\beta] - \text{Tr}[U_\alpha U_{\beta^{-1}}] = 0, \quad (2.16)$$

$$\mathcal{T}[\alpha] \mathcal{T}[\beta] + \mathcal{T}[\alpha \#_s \beta] + \mathcal{T}[\alpha \#_s \beta^{-1}] = 0, \quad (2.17)$$

$$\mathcal{T}[\alpha][\beta] + \mathcal{T}[\alpha \#_s \beta] + \mathcal{T}[\alpha \#_s \beta^{-1}] = 0; \quad (2.18)$$

namely the spinor identity (one  $+$  and two  $-$ ) has become a binor identity (all  $+$ ) (see Penrose [30]). While the first is non local, the second is local, and is the basic identity at the roots of binor calculus and  $A = -1$  recoupling theory. For the notations  $\circ$  and  $\#$  (to be used in a moment), see for instance [8].

We recall here, for later use, the retracing identity. For all loops  $\alpha$  and segments  $\gamma$ , we have [3]

$$\mathcal{T}[\alpha] = \mathcal{T}[\alpha \circ \gamma \circ \gamma^{-1}]. \quad (2.19)$$

The Poisson bracket algebra of these loop variables is easily computed. For a rigorous way of performing these computations, see [31]. We give here the Poisson bracket of the  $\mathcal{T}$  variables of order 0 and 1.

$$\begin{aligned}\{\mathcal{T}[\alpha], \mathcal{T}[\beta]\} &= 0, \\ \{\mathcal{T}^a[\alpha](s), \mathcal{T}[\beta]\} &= -G \Delta^a[\beta, s] \frac{1}{2} \{\mathcal{T}[\alpha \#_s \beta] - \mathcal{T}[\alpha \#_s \beta^{-1}]\},\end{aligned}\quad (2.20)$$

where we have defined:

$$\Delta^a[\beta, s] = \int_\beta d\tau \dot{\beta}^a(\tau) \delta^3[\beta(\tau), s]. \quad (2.21)$$

The factor  $-\frac{1}{2}$ , different than in previous papers, is due to the new conventions.

### III. THE LOOP REPRESENTATION OF QUANTUM GRAVITY

We now define the loop representation [32] of quantum gravity as a linear representation of the Poisson algebra of the  $\mathcal{T}$  variables. First, we define the carrier space of the representation. To this aim, we consider the linear subspace  $\mathcal{K}$  of the free loop algebra defined by

$$\mathcal{K} = \{\Phi \in \mathcal{A}^f[\mathcal{L}] \mid \mathcal{T}[\Phi] = 0\}, \quad (3.1)$$

and we define the carrier space  $\mathcal{V}$  of the representation by

$$\mathcal{V} = \mathcal{A}^f[\mathcal{L}]/\mathcal{K}. \quad (3.2)$$

In other words, the state space of the loop representation is defined as the space of the equivalence classes of linear combinations of multiloops, under the equivalence defined by the Mandelstam relations

$$\Phi \sim \Psi \text{ if } \mathcal{T}[\Phi] = \mathcal{T}[\Psi], \quad (3.3)$$

namely by the equality of the corresponding holonomies [9].<sup>2</sup> We denote the equivalence classes defined in this way, namely the elements of the quantum state space of the theory as Mandelstam classes, and we indicate them in Dirac notation as  $\langle \Phi |$ . Clearly, the multiloop states  $\langle \alpha |$  span (actually, overspan) the state space  $\mathcal{V}$ . Later we will define a scalar product on  $\mathcal{V}$ , and promote it to a Hilbert space. The reason for preferring a bra notation over a ket notation is just historical at this point. We recall that the loop representation was originally defined in terms of kets  $|\psi\rangle$  in the dual of  $\mathcal{V}$ . These are represented on the (overcomplete) basis  $\langle \alpha |$  by loop functionals

$$\psi(\alpha) = \langle \alpha | \psi \rangle. \quad (3.4)$$

The principal consequences of the Mandelstam relations are the following.

1. The element  $\langle \alpha |$  does not depend on the orientation of  $\alpha$ :  $[\alpha] \sim [\alpha^{-1}]$ .
2. The element  $\langle \alpha |$  does not depend on the parameterization of  $\alpha$ :  $[\alpha] \sim [\beta]$  if  $\beta^a(\tau) = \alpha^a(f(\tau))$ .
3. Retracing: if  $\gamma$  is a *segment* starting in a point of  $\alpha$  then.

$$[\alpha \circ \gamma \circ \gamma^{-1}] \sim [\alpha]. \quad (3.5)$$

4. Binor identity:

$$[\alpha] \cdot [\beta] \sim -[\alpha \#_s \beta] - [\alpha \#_s \beta^{-1}]. \quad (3.6)$$

It has been conjectured that all Mandelstam relations can be derived by repeated use of these identities. We expect that the methods described below may allow to prove this conjecture, but we do not discuss this issue here.

Next, we define the quantum operators corresponding to the  $\mathcal{T}$ -variables as linear operators on  $\mathcal{V}$ . These form a representation of the loop variables Poisson algebra. We define the loop operators as acting on the bra states  $\langle \Phi |$  from the right. (Since they act on the right, they define, more precisely, an *anti*-representation of the Poisson algebra.) We define the  $\hat{\mathcal{T}}[\alpha]$  operator by

$$\left\langle c_0 + \sum_i c_i [\alpha_i] + \sum_{ij} c_{ij} [\alpha_i][\alpha_j] + \dots \right| \hat{\mathcal{T}}[\alpha] = \left\langle c_0[\alpha] + \sum_i c_i [\alpha_i][\alpha] + \sum_{ij} c_{ij} [\alpha_i][\alpha_j][\alpha] + \dots \right|. \quad (3.7)$$

Next, we define the  $\hat{\mathcal{T}}^a[\alpha](s)$  operator. This is a derivative operator (i.e. it satisfies Leibniz rule) over the free loop algebra such that

$$\langle [\beta] | \hat{\mathcal{T}}^a[\alpha](s) = -il_0^2 \Delta^a[\beta, s] \frac{1}{2} (\langle [\alpha \#_s \beta] | - \langle [\alpha \#_s \beta^{-1}] |), \quad (3.8)$$

where we have introduced the elementary length  $l_0$  by

$$l_0^2 = \hbar G = \frac{16\pi \hbar G_{\text{Newton}}}{c^3} = 16\pi l_{\text{Planck}}^2. \quad (3.9)$$

---

<sup>2</sup> $\mathcal{T}[\Phi]$  is a function on configuration space, namely a function over the space of smooth connections. Equality between functions means of course having the same value for any value of the independent variable; here, for all (smooth) connections.

The definition extends on the entire free loop algebra by Leibniz rule and linearity. The two operators commute with the Mandelstam relations and are therefore well defined on  $\mathcal{V}$ .

Notice that the factor  $\Delta^a[\beta, s]$  in (3.8) depends on the orientation of the loop  $\beta$ : it changes sign if the orientation of  $\beta$  is reversed. So does the difference in the parentheses, therefore the r.h.s of (3.8) is independent from the orientation of  $\beta$ , as the l.h.s.. On the other hand, both the r.h.s and the l.h.s of (3.8) change sign if we reverse the orientation of  $\alpha$ .

The action of the  $\hat{\mathcal{T}}^a[\alpha](s)$  operator on a state  $\langle[\beta]|$  can be visualized graphically. The graphical action is denoted a “grasp”, and it can be described as follows: i. Disjoin the two edges of the loop  $\beta$  and the two edges of the loop  $\alpha$ , that enter the intersection point  $s$ . ii. Pairwise join the four open ends of  $\alpha$  and  $\beta$  in the two possible alternative ways. This defines two new states. Consider the difference between these two states (arbitrarily choosing one of the two as positive). iii. Multiply this difference by the factor  $-i l_0^2 \Delta^a[\beta, s]$ , where the direction of  $\beta$  (which determines the sign of  $\Delta^a[\beta, s]$ ) is determined as follows: it is the direction induced on  $\beta$  by  $\alpha$  (which *is* oriented) in the term chosen as positive. A moment of reflection shows that the definition is consistent, and independent from the choice of the positive term. An explicit computation shows that the operators defined realize a linear representation of the Poisson algebra of the corresponding classical observables.

The grasping rule generalizes to higher order  $\mathcal{T}$ -variables. The action of  $\hat{\mathcal{T}}^{a_1 \dots a_n}[\alpha](s_1, \dots, s_n)$ , over a single loop-state  $[\beta]$  is given as follows. First the result vanishes unless  $\beta$  crosses all the  $n$  points  $s_i$ . If it does, the action of  $\hat{\mathcal{T}}^{a_1 \dots a_n}[\alpha](s_1, \dots, s_n)$  is given by the simultaneous grasp on all intersection points. This action produces  $2^n$  terms. These terms are summed algebraically with alternate signs, and the result is multiplied by a factor  $-i l_0^2 \Delta^a[\beta, s_1]$  for each grasp, where the sign of each coefficient  $\Delta^a[\beta, s_i]$  is determined assuming that  $\beta$  is oriented consistently with  $\alpha$  in the term chosen as positive. Again, a moment of reflection shows that the definition is consistent, and independent from the choice of the positive terms. The generalization to arbitrary states, using linearity and the Leibniz rule, is straightforward. This concludes the construction of the linear ingredients of the loop representation.

#### IV. LOOP STATES AND RECOUPLING THEORY

A quantum state  $\langle\Phi|$  in the state space  $\mathcal{V}$  is a Mandelstam equivalence class of elements of the form (2.9). We now show that because of the equivalence relation, these states are related to tangles –in the sense of Kauffman [33]– and they obey the formal identities that define the Temperley-Lieb-Kauffman recoupling theory described in Ref. [24]. This fact yields two results. First, we can write a basis in  $\mathcal{V}$ . This basis is constructed in the next section. Second, recoupling theory becomes a powerful calculus in loop quantum gravity.

Consider the element  $\Phi$ , given in (2.9), of the vector space  $\mathcal{A}^f[\mathcal{L}]$ . We need some definitions.

**Graph of a state.** We denote the union in  $M$  of the images of all the loops in the r.h.s of (2.9) as the “graph of  $\Phi$ ”, and we indicate it as  $\Gamma_\Phi$ . Notice that  $\Gamma_\Phi$  is a graph in the sense of graph theory [34], embedded in  $M$ .

**Vertex.** We denote the points  $i$  where  $\Gamma_\Phi$  fails to be a smooth submanifold of  $M$  as “vertices”.

**Edge.** We denote the lines  $e$  of the graph connecting the vertices as “edges”.

**Valence.** We say that a vertex  $i$  has valence  $n$ , or is  $n$ -valent, if  $n$  edges are adjacent to it. A vertex can have any positive integer valence, including 1 and 2.

Clearly,  $\Phi$  is not uniquely determined by its graph  $\Gamma_\Phi$ . If our only information about a state is its graph, then we do not know how the state is decomposed into multiloops, nor how many single loops run along each edge, nor how the single loops are rooted through the vertices. We now introduce a graphical technique to represent this missing information. The technique is based on the idea of “blowing up” the graph –as if viewed through an infinite magnifying glass– and representing the additional information in terms of planar tangles on the blown up graph. As we will see, these tangles obey recoupling theory.

First, draw a graph isomorphic to  $\Gamma_\Phi$  in the sense of graph theory (that is, the isomorphism preserves only adjacency relations between vertices and edges), on a two dimensional surface. As usual in graph theory, we must distinguish points representing vertices from accidental intersections between edges generated by the fact that we are representing a non-planar graph on a plane. Denote these accidental intersections as “false intersections”. Next, replace each vertex (not the false intersections) by (the interior of) a circle in the plane, and each edge by a ribbon connecting two circles. (At false intersections, ribbons bridge each other without merging.) In this way, we construct a “thickened out” graph: a two-dimensional oriented surface which (loosely speaking) has the topology of the graph  $\Gamma_\Phi$  times the  $[0, 1]$  interval.

**Ribbon-net.** We call this two-dimensional surface the “ribbon-net” (or simply the ribbon) of the graph  $\Gamma_\Phi$ , and we denote it as  $R_\Phi$ . Notice that the graph  $\Gamma_\Phi$  is embedded in  $M$ , while its ribbon-net  $R_\Phi$  is not.

Now we can represent the missing information needed to reconstruct  $\Phi$  from  $\Gamma_\Phi$  as (a formal linear combination of) tangles drawn on the surface  $R_\Phi$ . First, we represent each multiloop in (2.9) by means of a closed line over  $R_\Phi$ :

**Planar (representation of a) multiloop.** For each loop  $\alpha_i$  in a given multiloop  $\alpha$  we draw a loop  $\alpha_i$  over the ribbon-net  $R_\Phi$ , wrapping around  $R_\Phi$  in the same way in which  $\alpha_i$  wraps around  $\Gamma_\Phi$ . We denote the drawing (over  $R_\Phi$ ) of all the loops of a multiloop as “the planar representation” of the multiloop  $\alpha$ , or simply as the “planar multiloop”. We indicate it as  $P_\alpha$ .

For technical reasons, we allow edges and vertices of the ribbon-net to be empty of loops as well. Thus, we identify a ribbon-net containing a planar multiloop, with a second one obtained from the first by adding edges and vertices empty of loops. Finally:

**Planar (representation of a) state.** Every state  $\langle\Phi|$  is a formal linear combination of multiloops:  $\langle\Phi| = \sum_j c_j [\alpha_j]$  (up to equivalence). We denote the corresponding formal linear combination  $P_\Phi = \sum_j c_j P_{\alpha_j}$  of planar multiloops on the ribbon-net  $R_\Phi$  (up to equivalence), as a planar representation of  $\langle\Phi|$ .

We have split the information contained in  $\Phi$  in two parts:  $\Phi$  determines a graph  $\Gamma_\Phi$  embedded in  $M$  and a planar state  $P_\Phi$ .  $P_\Phi$  is a linear combinations of drawings of loops over a surface (the ribbon-net  $R_\Phi$ ) and codes the information on which loops are present and how they are rooted through intersections. This information is *purely combinatorial*. On the other hand,  $\Gamma_\Phi$  contains the information on how the loops are embedded into  $M$ .

Notice that a multiloop determines its planar representation only up to smooth planar deformations of the lines within the circles and the ribbons of the ribbon-net. In other words, we can arbitrarily deform the lines within each circle and within each ribbon, without changing  $\Phi$ . In particular, the lines of the planar representation will intersect in points of  $R_\Phi$ , and we can apply Reidemeister [35] moves [33] to such intersections (that is, disentangle them). Under- and over-crossings of loops within  $R_\Phi$  are not distinguished.

Let us come to the key observation on which the possibility of using recoupling theory relies. Consider an element  $\Phi$  of the free vector algebra. For simplicity, let us momentarily assume that  $\Phi$  is formed by a single loop  $\Phi = [\alpha]$  (which may self-intersect and run over itself). Thus  $\Phi = (\Gamma_\alpha, P_\alpha)$ . Consider an intersection of two lines (two segments of  $P_\alpha$ ) in  $R_\Phi$ . Break the two lines meeting at this intersection, and pairwise rejoin the four legs, in the two alternative possible ways, as in Figure 1.

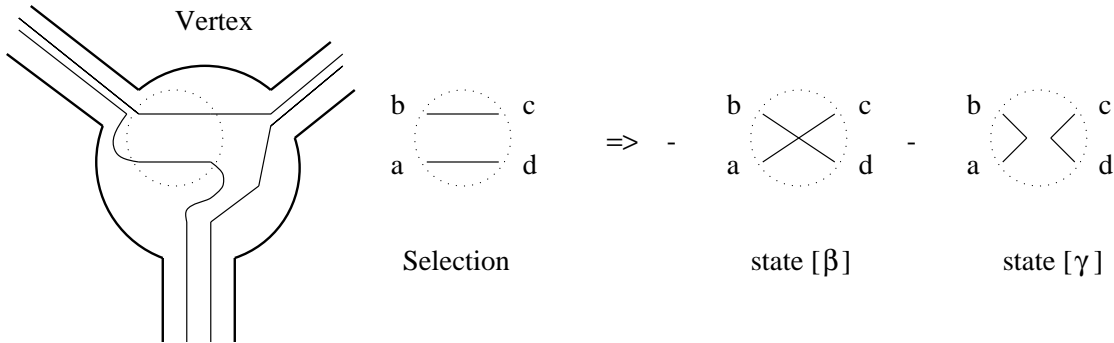


FIG. 1. The binor identity.

We obtain two new loops on  $R_\Phi$ , which we denote as  $P_{[\beta]}$  and  $P_{[\gamma]}$ . Consider the element  $\Psi$  of the free vector algebra uniquely determined by the graph  $\Gamma_\Psi = \Gamma_\Phi$ , and by the linear combination of planar representations  $P_\Psi = -P_\beta - P_\gamma$ . Notice that  $\Psi$  is different than  $\Phi$  as an element of the free vector algebra; however, the two are in the same Mandelstam equivalence class because of the binor relation (3.6), and therefore they define the same element of the quantum state space  $\mathcal{V}$ . Namely  $\langle\Psi| = \langle\Phi|$ . We say that two planar representations  $P_\Phi$  and  $P_\Psi$  are “equivalent” if  $\langle\Psi| = \langle\Phi|$ . Thus, in dealing with planar representations of a quantum state  $\langle\Phi|$ , we can freely use the identity

$$\times = - \left| \right| - \cup \quad (4.1)$$

on  $P_\Phi$  without changing the quantum state. This identity is the identity (i) in page 7 of reference [24], (equation (B1) in Appendix B) which is the key axiom of recoupling theory – with the value of the  $A$  parameter set to  $-1$ .

An easy to derive consequence is that every closed line entirely contained within a circle, or within a ribbon, can be replaced by a factor  $d = -2$ . Furthermore, it is easy to see that the retracing identity (3.5) implies that the loops of  $P_\Phi$  can be arbitrarily deformed within the *entire* ribbon-net, without changing the state  $\langle\Phi|$ . In particular, every loop contractible in  $R_\Phi$  can be replaced by a factor  $d = -2$ . This is the second axiom of recoupling theory (equation (B2) in Appendix B) in the  $A = -1$  case. The value  $A = -1$ , correspond to the case in which the distinction between over- and under-crossings can be neglected, consistently with the fact such distinction is irrelevant for the planar representation of a loop.

Thus  $P_\Phi$  can be interpreted as a linear combination of tangles in the sense of reference [24]. The tangles obey the axioms of recoupling theory. They are confined inside the oriented surface  $R_\Phi$  with has a highly nontrivial topology. This is the key result of this section.

The relation between loop states and recoupling theory is subtle, and may generate confusion. A source of confusion is given by the fact that the relation between recouplings and knots in knot theory [24] is different from the relation between recouplings and knots in quantum gravity. In both cases recouplings enters as a consequence of a skein (or binor) equation –as equation (4.1)– holding at intersections. But in knot theory this equation is satisfied by the Kauffman brackets at the “false intersections” of the planar projection of a loop. Contrary to this, in quantum gravity equation (4.1) *does not hold* for the false intersections. It holds for the intersections of lines *within*  $R_\Phi$ .

On the other hand, knots play a role in quantum gravity as well [2], because of the diffeomorphism constraint. GR’s diffeomorphism invariance identifies states that have equivalent  $P_\Phi$ , and whose *graphs* can be deformed into each other by 3-d diffeomorphisms of  $M$  in the connected component of the identity. To clarify this point, let us require that the ribbon-net  $R_\Phi$  is generated by a two dimensional projection of  $\Gamma_\Phi$ , and let us keep track of the resulting over- and under- crossings at false intersections. Then diffeomorphism invariance identifies all states that have equivalent  $P_\Phi$ , and whose ribbon-nets can be transformed into each other by Reidemeister moves *at the false intersections*. Thus, as far as diff-invariant states are concerned, Reidemeister moves can be used at the tangles’ intersections *within the ribbon-net* as well as at the false intersections. But in the first case a skein equation (equation (4.1)) holds, in the second it doesn’t.<sup>3</sup> Mixing up the two cases has generated a certain confusion in the past.

An immediate consequence of the result is that we can write a basis in  $\mathcal{V}$  following [24]. Given a state  $\langle\Psi|$ , and its ribbon-net  $R_\Phi$ , we can use (4.1) to eliminate all intersections from the  $P_\alpha$  of each multiloop. Next, we can retrace each single line that returns over itself, and eliminate every loop contractible in  $R_\Phi$ . We obtain parallel lines without intersections along each ribbon and routings without intersections at each vertex. No further use of the retracing or binor identity is then possible without altering this form. This procedure defines a basis of independent states, labeled by the graph, the number of lines along each edge, and elementary routings at each node. An elementary routing is a planar rooting of loops through the vertex of the ribbon-net, having no intersections. This basis is not very practical for calculations. In the next section, we use the technology of [24] to define a more useful basis.<sup>4</sup>

## V. THE SPIN NETWORK BASIS

The representation  $(\Gamma_\Phi, P_\Phi)$  of a state  $\langle\Phi|$  can be expanded in terms of a “virtual” trivalent representation as follows.

**Virtual graph.** To every graph  $\Gamma$ , we can associate a trivalent graph  $\Gamma^v$  as follows. For each  $n$ -valent vertex  $v$  of  $\Gamma$ , (arbitrarily) label the adjacent edges as  $e_0 \dots e_{(n-1)}$ , and disjoin them from  $v$ . Then, replace  $v$  with  $n - 2$  trivalent

---

<sup>3</sup>This is true in general. One may wonder if there is any special quantum state  $\langle\Phi_0|$  for which the relation (4.1) holds at false intersections as well. The possibility that such a special state could exist in quantum gravity has been explored, with various motivations, by various authors [26,36].

<sup>4</sup>A basis in a linear space is a set of linearly independent vectors that span the linear space. The fact we work in linear spaces without fixing a scalar product (we will fix a scalar product only later, in section VIII) has raised some confusion in the past. It is perhaps worthwhile recalling that the notions of basis, eigenvalues and eigenvectors are well defined notions for linear spaces, not just for Hilbert spaces. (They do not require a scalar product to be defined in order to make sense.) Similarly, the fact that a linear operator is diagonalizable, or has real eigenvalues does not depend on the presence of a scalar product. Given an arbitrary linear basis  $v_i$  in a finite dimensional linear space, a linear operator  $A$  is hermitian in this basis if its matrix elements (defined by  $(Av)_i = A_i^j v_j$ ) satisfy  $A_i^j = \bar{A}_j^i$ . If  $A$  is hermitian in a basis, then  $A$  is diagonalizable and has real eigenvalues. This is true independently from any scalar product.



vertices  $N_1 \dots N_{n-2}$ , denoted “virtual” vertices. Join the virtual vertices with  $n - 3$  “virtual” edges  $E_2 \dots E_{n-2}$ , where  $E_i$  joins  $N_{i-1}$  and  $N_i$ . Prolong the edges  $e_2 \dots e_{(n-1)}$  to reach the corresponding virtual vertices  $N_1 \dots N_{n-2}$ , and the edges  $e_1$  and  $e_{(n-1)}$  to reach the virtual vertices  $N_1$  and  $N_{n-2}$ . Denote the resulting trivalent graph  $\Gamma^v$  as the virtual graph associated to  $\Gamma$  (for the chosen ordering of edges).

**Virtual ribbon-net.** We denote the ribbon-net of  $\Gamma_\Phi^v$  as the virtual ribbon-net  $R_\Phi^v$  of  $\Phi$ . We view it as a subset of  $R_\Phi$ , namely we view the virtual circles  $N_1 \dots N_{n-2}$  and the virtual ribbons  $E_2 \dots E_{n-2}$  as drawn inside the circle  $c$  representing  $v$ . This circle  $c$  indicates that the virtual vertices  $N_1 \dots N_{n-2}$  correspond all to the same point of  $M$ . (Thus, a virtual ribbon-net is a trivalent ribbon-net with strings of adjacent intersections specified.)

**Virtual representation.** Finally, deform  $P_\Phi$  so that it lies entirely inside  $R_\Phi^v$ . We indicate the deformed  $P_\Phi$  as  $P_\Phi^v$ , and call it the “virtual” planar representation of  $\Phi$ . The virtual representation  $P_\Phi^v$  of a state is not unique, due to the arbitrariness of assigning the ordering  $e_0 \dots e_{(n-1)}$  to the edges of  $n$ -valent intersections.

The above construction is more difficult to describe in words than to visualize, and is illustrated in Figure 2.

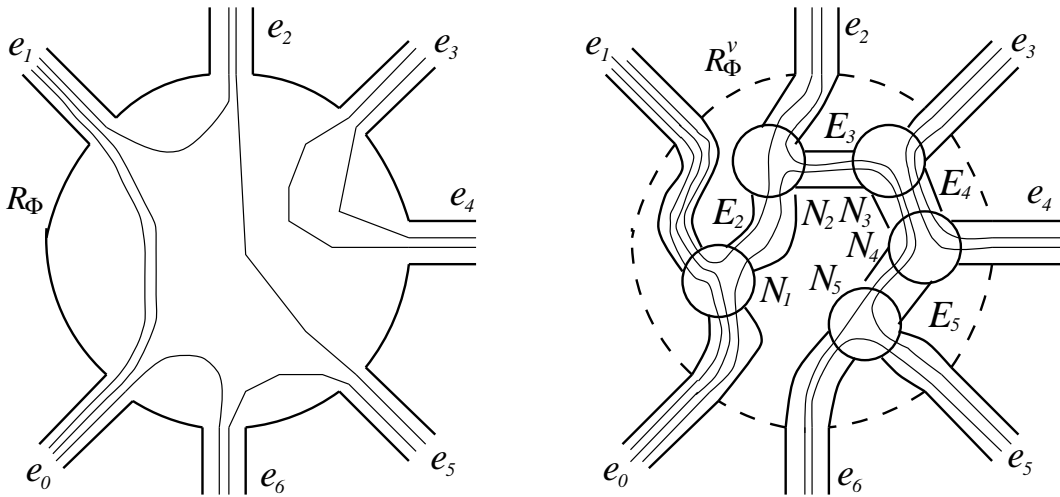


FIG. 2. Construction of “virtual” vertices and “virtual” strips over an  $n$ -valent vertex.

Consider now deformations of the tangle  $P_\Phi^v$  within  $R_\Phi^v$  – a subset of the deformations within the full  $R_\Phi$ . We can move all intersections of deform  $P_\Phi^v$  away from the vertices (to the virtual or real ribbons), leaving trivalent vertices free from intersections. Next, we can use the binor relation to remove all intersections from the ribbons, leaving non-intersecting tangles with  $n$  inputs and  $n$  outputs along each single ribbon  $e$ . As described in Sec 2.2 of [24], tangles of this kind can be described as elements of the (tangle-theoretic) Temperley-Lieb algebras  $T_n^{(e)}$ . A basis of this algebra is obtained by using the Jones-Wenzl projectors  $\Pi_n^{(e)}$ . Since we are here in the case  $A = -1$ , the  $\Pi_n^{(e)}$  are just normalized antisymmetrizers. More precisely, given the multiloop  $P_\alpha$  with  $n$  lines along the ribbon  $e$ , call  $P_\alpha^{(p)}$ ,  $p = 1 \dots n!$  the multiloops obtained by all possible permutations  $p$  in the way the  $n$  lines entering  $e$  are connected to the  $n$  outgoing lines, and  $|p|$  the parity of the permutation, then

$$\Pi_n^{(e)} P_\alpha = \frac{1}{n!} \sum_p (-1)^{|p|} P_\alpha^{(p)}. \quad (5.1)$$

Notice the  $1/n!$  factor, which was not present in previous conventions [14]. It follows from the completeness of the Jones-Wenzel projectors that a basis for all planar loops over a given  $R_\Phi^v$  is given by the linear combination of loops in which the lines along each (virtual and real) edge are fully antisymmetrized. We can therefore expand every state in states in which lines are fully antisymmetrized along each ribbon. A state in which the lines along each (virtual or real) ribbon are fully antisymmetrized is a spin network state. Thus, we recover the result of reference [10], to which we refer for details.

A spin network state is characterized by a graph  $\Gamma$  in  $M$ , by the assignment of an ordering to the edges adjacent to each vertex, and by the number  $p_e$  of (antisymmetrized) lines in each virtual or real edge  $e$ . We denote the integer  $p_e$

as the “color” of the corresponding edge  $e$  of  $\Gamma^v$ . We will use also the “spin”  $j_e$  of the edge, defined as half its color:  $j_e = \frac{1}{2}p_e$ .<sup>5</sup> At each vertex, the colors  $p_1$ ,  $p_2$  and  $p_3$  of the three adjacent edges satisfy a compatibility condition: there must exist three positive integers  $a$ ,  $b$  and  $c$  (the number of lines rooted through each pair of edges) such that

$$p_1 = a + b, \quad p_2 = b + c, \quad p_3 = c + a, \quad (5.2)$$

It is easy to see that this condition is equivalent to the Clebsch-Gordon condition that each of the three  $su(2)$  representations of spin  $j_i = 1/2 p_i$  is contained in the tensor product of the other two [30].

The spin network states form a basis in  $\mathcal{V}$ . The basis elements are given as follows. For every graph  $\Gamma$  embedded in  $M$ , choose an ordering of the edges at each node. This choice associates an oriented trivalent virtual graph  $\Gamma^v$  (non-embedded) to every  $\Gamma$ .

**Spin network.** A spin network  $S$  is given by a graph  $\Gamma_S$  in  $M$ , and by a compatible coloring  $\{p_e\}$  of the associated oriented trivalent virtual graph  $\Gamma^v$ . Thus  $S = (\Gamma_S, \{p_e\})$ .

**Spin network state.** For every spin network  $S$ , the spin network quantum state  $\langle S| = (\Gamma_S, P_S)$  is the element of  $\mathcal{V}$  determined by the graph  $\Gamma_S$  and by the linear combination  $P_S$  of planar multiloops obtained as follows. Draw  $p_e$  lines on each ribbon  $e$  of the ribbon-net  $R_S^v$ ; connect lines at intersections without crossings; this gives a planar multiloop  $P_S^{(0)}$ ; then

$$P_S = \prod_{e \in \Gamma} \Pi_{p_e}^{(e)} P_S^{(0)}. \quad (5.3)$$

We can represent a spin network state as a colored trivalent graph over the ribbon-net  $R_S^v$  (with a single edge along each ribbon). This representation satisfies the identities of recoupling theory. We describe the main ones of these identities in Appendix E. As an example, we give here the formula that allows one to express the basis elements of a 4-valent intersection in terms of the basis elements of a different trivalent expansion. Using the recoupling theorem of [24] (pg. 60), we have immediately

$$\begin{array}{c} b \quad c \\ \diagdown \quad \diagup \\ \bullet \\ \diagup \quad \diagdown \\ a \quad d \end{array} \quad \begin{array}{c} j \\ \diagdown \quad \diagup \\ \bullet \\ \diagup \quad \diagdown \\ a \quad d \end{array} = \sum_i \left\{ \begin{array}{ccc} a & b & i \\ c & d & j \end{array} \right\} \begin{array}{c} b \quad c \\ \diagdown \quad \diagup \\ \bullet \\ \diagup \quad \diagdown \\ a \quad d \end{array} \quad \begin{array}{c} i \\ \diagdown \quad \diagup \\ \bullet \\ \diagup \quad \diagdown \\ a \quad d \end{array} \quad (5.4)$$

where the quantities  $\left\{ \begin{array}{ccc} a & b & i \\ c & d & j \end{array} \right\}$  are  $su(2)$  six-j symbols (normalized as in [24]; see Appendices).

A side remark should be added. An embedded colored trivalent graph specifies a state  $\Phi$  only up to a global sign, because it does not fix the overall sign of the antisymmetrized linear combination of multiloops. To keep track of this overall sign, one needs *oriented* trivalent graphs, as in reference [30] where Penrose considered oriented spin networks and in [10]. An orientation of a trivalent graph is an assignment of a cyclic order to the edges of each node, modulo  $Z_2$  (that is, identifying two orientations if they differ in an even number of intersections).  $\Gamma^v$  is oriented by the order assigned to the edges entering each vertex, and ribbon-nets are oriented (consistently, we assume) as graphs because they are oriented as two-surfaces: edges can be ordered –say– clockwise.

### A. The Action of the operators in the spin-network basis

We now describe how the  $\hat{\mathcal{T}}$  operators act on the spin network states. From Eq. (3.7), the operator  $\hat{\mathcal{T}}[\alpha]$ , acting on a state  $\langle \Phi|$  simply adds a loop to  $\langle \Phi|$ . Consider the graph  $\Gamma$  formed by the union (in  $M$ ) of the graphs of  $\Phi$  and  $\alpha$ . Since we admit empty edges, we can represent  $\Phi$  over the ribbon-net  $R$  associated to  $\Gamma$ . In this representation, the action of  $\hat{\mathcal{T}}[\alpha]$  consists in adding the draw of  $\alpha$  over  $R$ . Using the expression for the Jones-Wenzl projectors in [24] (pg. 96), one can expand the non-antisymmetrized lines, if any, in combinations of antisymmetrized ones.

---

<sup>5</sup>The oscillation between the historically motivated half integer terminology “spin” and the rationally motivated integer terminology “color” goes back to Penrose’s papers on spin networks [30].

Higher order loop operators are expressed in terms of the elementary grasp operation, Eq. (3.8). The ribbon construction allows us to represent the grasp operation in a simpler form. Indeed, one easily sees that Eq. (3.8) is equivalent to the following: acting on an edge with color 1, the grasp creates two virtual trivalent vertices (inside the same circle, corresponding to the intersection point) – one on the spin-network state and one on the loop of the operator. The two vertices are joined by a virtual strip of color 2, and the overall multiplicative factor is determined as follows. The sign of the tangent of  $\beta$  in  $\Delta^a[\beta, s]$  is determined by the orientation of  $\beta$  consistent with the positive-terms of the loop expansion of the spin network. The equivalence between the old definition of the grasp and the new one is illustrated in Figure 3.

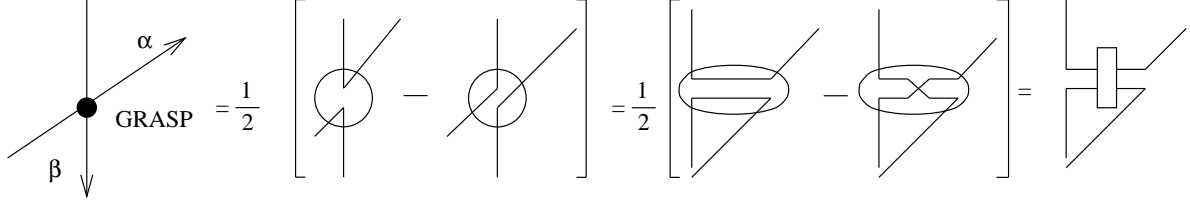


FIG. 3. Action of the grasp.

A straightforward computation, using Leibnitz rule, shows that acting on an edge with color  $p$ , the grasp has the very same action, with the multiplicative factor multiplied by  $p$ . Finally, notice that the two antisymmetrized loops form a (virtual) spin network edge of color 2. Therefore, we can express the action of the grasp in the spin network basis by the following equation

$$\begin{array}{c} \beta \downarrow \\ | \\ s \\ \text{GRASP} \\ | \\ p \end{array} \begin{array}{c} \nearrow \alpha \\ \nearrow \end{array} = p \Delta^a[\beta, s] \quad (5.5)$$

This simple form of the action of the loop operators on the spin-network basis is the reason that enables us to use recoupling-theory in actual calculations involving quantum gravity operators. Notice that it is the ribbon-net construction that allows us to “open up” the intersection point and represent it by means of two vertices (one over  $\alpha$  and one over  $\beta$ ) and a (“zero length”) edge connecting the two vertices. These two vertices and this edge are all in the same point of the three-manifold  $M$ .

Higher order loop operators act similarly, as sketched in Figure 4.

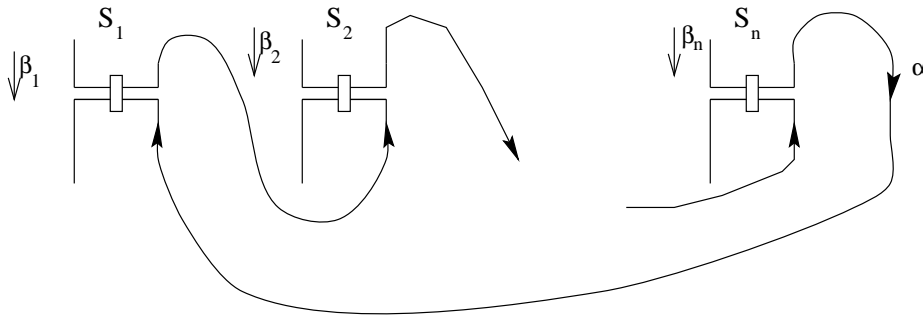


FIG. 4. Representation of the  $n$  grasp of the  $\mathcal{T}^{a_1 \dots a_n}[\alpha](s_1, \dots, s_n)$  operator.

## VI. THE AREA OPERATOR

A surface  $\Sigma$  in  $M$  is an embedding of a 2-dimensional manifold  $\Sigma$ , with coordinates  $\sigma^u = (\sigma^1, \sigma^2)$ ,  $u, v = 1, 2$ , into  $M$ . We write  $S : \Sigma \rightarrow M^3, \sigma^u \rightarrow x^a(\sigma)$ . The metric and the normal one form on  $\Sigma$  are given by

$$g^\Sigma = S^* g, \quad g_{uv}^\Sigma = \frac{\partial x^a}{\partial \sigma^u} \frac{\partial x^b}{\partial \sigma^v} g_{ab}; \quad (6.1)$$

$$n_a = \frac{1}{2} \epsilon^{uv} \epsilon_{abc} \frac{\partial x^b}{\partial \sigma^u} \frac{\partial x^c}{\partial \sigma^v}. \quad (6.2)$$

The area of  $\Sigma$  is

$$\begin{aligned} A[\Sigma] &= \int_\Sigma d^2\sigma \sqrt{\det g^\Sigma} = \int_\Sigma d^2\sigma \sqrt{\frac{1}{2} \epsilon^{u\bar{u}} \epsilon^{\bar{v}v} g_{uv}^\Sigma g_{\bar{u}\bar{v}}^\Sigma} \\ &= \int_\Sigma d^2\sigma \sqrt{n_a n_b \tilde{E}^{ai} \tilde{E}_i^b}, \end{aligned} \quad (6.3)$$

where we have used

$$\begin{aligned} \epsilon^{u\bar{u}} \epsilon^{\bar{v}v} g_{uv}^\Sigma g_{\bar{u}\bar{v}}^\Sigma &= \epsilon^{u\bar{u}} \epsilon^{\bar{v}v} \frac{\partial x^a}{\partial \sigma^u} \frac{\partial x^b}{\partial \sigma^v} g_{ab} \frac{\partial x^{\bar{a}}}{\partial \sigma^{\bar{u}}} \frac{\partial x^{\bar{b}}}{\partial \sigma^{\bar{v}}} g_{\bar{a}\bar{b}}, \\ \epsilon^{u\bar{u}} \frac{\partial x^a}{\partial \sigma^u} \frac{\partial x^{\bar{a}}}{\partial \sigma^{\bar{u}}} &= \frac{1}{2} \epsilon^{u\bar{u}} \frac{\partial x^{a'}}{\partial \sigma^u} \frac{\partial x^{\bar{a}'}}{\partial \sigma^{\bar{u}}} \epsilon_{a'\bar{a}'c} \epsilon^{a\bar{a}c} = n_c \epsilon^{a\bar{a}c}, \\ gg^{c\bar{c}} &= \frac{1}{2} \epsilon^{a\bar{a}c} \epsilon^{b\bar{b}\bar{c}} g_{ab} g_{\bar{a}\bar{b}}. \end{aligned}$$

(On the role of played by surface area in the Ashtekar's formulation of GR, see [37].) We want to construct the quantum area operator  $\hat{A}[\Sigma]$ , namely a function of the loop representation operators whose classical limit is  $A[\Sigma]$ . Following conventional quantum field theoretical techniques, we deal with operator products by defining  $\hat{A}[\Sigma]$  as a limit of regularized operators  $\hat{A}_\epsilon[\Sigma]$  that do not contain operator products. The difficulty in the present context is to find a regularization that does not break general covariance. This can be achieved by a geometrical regularization [13,38].

Following [14], we begin by constructing a classical regularized expression for the area, namely a one parameter family of classical functions of the loop variables  $A_\epsilon[\Sigma]$  which converges to the area as  $\epsilon$  approaches zero. Consider a small region  $\Sigma_\epsilon$  of the surface  $\Sigma$ , whose coordinate area goes to zero with  $\epsilon^2$ . For every  $s$  in  $\Sigma$ , the smoothness of the classical fields implies that  $\tilde{E}^a(s) = \tilde{E}^a(x_I) + O(\epsilon)$ , where  $x_I$  is an arbitrary fixed point in  $\Sigma_\epsilon$ . Also,  $U_\alpha(s, t)_A^B = \mathbb{1}_A^B + O(\epsilon)$  for any  $s, t \in \Sigma_I$  and  $\alpha$  a (coordinate straight) segment joining  $s$  and  $t$ . It follows that (because of (A1)) to zeroth order in  $\epsilon$

$$\begin{aligned} \mathcal{T}^{ab}[\alpha_{st}](s, t) &= -\text{Tr} \left[ \tilde{E}^a(s) U_\alpha(s, t) \tilde{E}^b(t) U_\alpha(t, s) \right] \\ &= 2 \tilde{E}^{ai}(x_I) \tilde{E}_i^b(x_I). \end{aligned} \quad (6.4)$$

Using this, we can write

$$\epsilon^4 \tilde{E}^{ai}(x_I) \tilde{E}_i^b(x_I) = \frac{1}{2} \int_{\Sigma_\epsilon} d^2\sigma n_a(\sigma) \int_{\Sigma_\epsilon} d^2\tau n_b(\tau) \mathcal{T}^{ab}[\alpha_{\sigma\tau}](\sigma, \tau) + O(\epsilon), \quad (6.5)$$

where  $\alpha_{\sigma\tau}$  is, say, a (coordinate) circular loop with the two points  $\sigma$  and  $\tau$  on antipodal points. Next, consider the area of the full surface  $\Sigma$ . By the very definition of Riemann integral, (6.3) can be written as

$$A[\Sigma] = \int_\Sigma d^2\sigma \sqrt{n_a n_b \tilde{E}^{ai} \tilde{E}_i^b} = \lim_{\substack{N \rightarrow \infty \\ \epsilon \rightarrow 0}} \sum_{I_\epsilon} \epsilon^2 \sqrt{n_a(x_I) n_b(x_I) \tilde{E}^{ai}(x_I) \tilde{E}_i^b(x_I)} \quad (6.6)$$

where, following Riemann, we have partitioned the surface  $\Sigma$  in  $N$  small surfaces  $\Sigma_{I_\epsilon}$  of coordinate area  $\epsilon^2$  and  $x_I$  is an arbitrary point in  $\Sigma_{I_\epsilon}$ . The convergence of the limit to the integral, and its independence from the details of the construction, are assured by the Riemann theorem for all bounded smooth fields. Inserting (6.5) in (6.6), we obtain the desired regularized expression for the classical area, suitable to be promoted to a quantum loop operator

$$A[\Sigma] = \lim_{\epsilon \rightarrow 0} A_\epsilon[\Sigma] \quad , \quad (6.7)$$

$$A_\epsilon[\Sigma] = \sum_{I_\epsilon} \sqrt{A_{I_\epsilon}^2} \quad , \quad (6.8)$$

$$A_{I_\epsilon}^2 = \frac{1}{2} \int_{\Sigma_{I_\epsilon} \otimes \Sigma_{I_\epsilon}} d^2\sigma d^2\tau \, n_a(\sigma) n_b(\tau) \, \mathcal{T}^{ab}[\alpha_{\sigma\tau}](\sigma, \tau). \quad (6.9)$$

Notice that the powers of the regulator  $\epsilon$  in (6.5) and (6.6) combine nicely, so that  $\epsilon$  appears in (6.7) only in the integration domains.

We are now ready to define the area operator:

$$\hat{A}[\Sigma] = \lim_{\epsilon \rightarrow 0} \hat{A}_\epsilon[\Sigma], \quad (6.10)$$

$$\hat{A}_\epsilon[\Sigma] = \sum_{I_\epsilon} \sqrt{\hat{A}_{I_\epsilon}^2}, \quad (6.11)$$

$$\hat{A}_{I_\epsilon}^2 = \frac{1}{2} \int_{\Sigma_{I_\epsilon} \otimes \Sigma_{I_\epsilon}} d^2\sigma d^2\tau \, n_a(\sigma) n_b(\tau) \, \hat{\mathcal{T}}^{ab}[\alpha_{\sigma\tau}](\sigma, \tau). \quad (6.12)$$

The meaning of the limit in (6.10) needs to be specified. The specification of the topology in which the limit is taken is an integral part of the definition of the operator. As it is usual for limits involved in the regularization of quantum field theoretical operators, the limit cannot be taken in the Hilbert space topology where, in general, it does not exist. The limit must be taken in a topology that “remembers” the topology in which the corresponding classical limit (6.7) is taken. This is easy to do in the present context. We say that a sequence of (multi) loops  $\alpha_\epsilon$  converges to  $\alpha$  if  $\alpha_\epsilon$  converges pointwise to  $\alpha$ ; we say that a sequence of quantum states  $\langle \alpha_\epsilon |$  converges to the state  $\langle \alpha |$  if  $\alpha_\epsilon \rightarrow \alpha$  for at least one  $\alpha_\epsilon \in \langle \alpha_\epsilon |$  ( $\forall \epsilon$ ) and one  $\alpha \in \langle \alpha |$ . This definition extends immediately to general states  $\langle \Phi |$  by linearity, and defines a topology on the state space, and the corresponding operator topology:  $\hat{O}_\epsilon \rightarrow \hat{O}$  iff  $\langle \Phi | \hat{O}_\epsilon \rightarrow \langle \Phi | \hat{O}$ ,  $\forall \langle \Phi |$ . Notice that the above is equivalent to say that  $\langle \Phi_\epsilon |$  converges to  $\langle \Phi |$  if  $\mathcal{T}[\Phi_\epsilon]$  converges pointwise to  $\mathcal{T}[\Phi]$ , which is the topology implicitly used in [18] to regularize the area operator.

An important consequence of the use of this topology is the following. Let  $\langle \Phi_\epsilon |$  converge to  $\langle \Phi |$ . Then the graphs  $\Gamma_{\Phi_\epsilon}$  converge to  $\Gamma_\Phi$  in the topology of  $M$ . In other words, given a  $\delta$ -neighborhood of  $\Gamma_\Phi$ , there exists an  $\epsilon$  such that  $\Gamma_{\Phi_\epsilon}$  is included in the  $\delta$ -neighborhood for all  $\epsilon' < \epsilon$ . Visually, we can imagine that the ribbon-nets  $R_{\Phi_\epsilon}$  “merge” into the ribbon-net  $\Gamma_\Phi^{ex}$  as  $\epsilon$  approaches zero. In addition, the representations  $P_{\Phi_\epsilon}$  go to  $P_\Phi$ , up to equivalence. This fact allows us to separate the study of a limit in two steps. First, we study of the graph of the limit state. In this process, the representations  $P_{\Phi_\epsilon}$  are merged into the ribbon-net  $R$  of the limit state. Second, we can use recoupling theory on  $R$ , in order to express the limit representation in terms of the spin network basis.

We now study the action of the area operator  $\hat{A}[\Sigma]$  given in (6.10) on a spin network state  $\langle S |$ . Namely, we compute  $\langle S | \hat{A}[\Sigma]$ . Let  $S \cap \Sigma$  be the set of the points  $i$  in the intersection of  $\Gamma_S$  and  $\Sigma$ . In other words, we label by an index  $i$  the points where the spin network graph  $\Gamma_S$  and the surface  $\Sigma$  intersect. Generically  $S \cap \Sigma$  is numerable, and does not include vertices of  $S$ . Here we disregard spin networks that have a vertex lying on  $\Sigma$  or a continuous number of intersection points with  $\Sigma$ . It was pointed out by A. Ashtekar that spin networks with a vertex *and* one -or more- of its adjacent edges lying on  $\Sigma$  are eigenstates of the area with eigenvalues that are not included in the spectrum of the operator computed in [14] -and derived again below. Therefore the spectrum of the area given in [14] is not complete. The physical relevance of these “degenerate” cases is unclear to us.

For small enough  $\epsilon$ , each intersection  $i$  will lie inside a distinct  $\Sigma_{I_\epsilon}$  surface.<sup>6</sup> Let us call  $\Sigma_{i_\epsilon}$  the surface containing the intersection  $i$  (at every fixed  $\epsilon$ ), and  $e_i$  the edge through the intersection  $i$ . Notice that  $\langle S | \hat{A}_{\Sigma_{I_\epsilon}}^2$  vanishes for all surfaces  $I_\epsilon$  except the ones containing intersections. Thus the sum over surfaces  $\sum_{I_\epsilon}$  reduces to a sum over intersections. Bringing the limit inside the sum and the square root, we can write

---

<sup>6</sup>The (perhaps cavilling) issue that an intersection may fall on the *boundary* between two  $I_\epsilon$  surfaces has been raised. This eventuality, however, does not generate difficulties for the following reason. The integrals we are using are not Lebesgue integrals, because, due to the presence of the  $\delta$ 's, regions of zero measure of the integration domain cannot be neglected – nor doubly counted. Therefore in selecting the partition of  $\Sigma$  in the  $I_\epsilon$  surfaces one must include each boundary in one and only one of the two surfaces (which are therefore partially open and partially closed). Boundary points are then normal points that fall inside one and only one integration domain.

$$\langle S | \hat{A}[\Sigma] = \sum_{i \in \{S \cap \Sigma\}} \langle S | \sqrt{\hat{A}_i^2} \quad (6.13)$$

$$\hat{A}_i^2 = \lim_{\epsilon \rightarrow 0} \hat{A}_{i_\epsilon}^2 \quad (6.14)$$

For finite  $\epsilon$ , the state  $\langle S | \hat{A}_{i_\epsilon}^2$  has support on the union of the graphs of  $S$  and the graph of the loop  $\alpha_{\sigma\tau}$  in the argument of the operator (6.12). But the last converges to a point on  $\Gamma_S$  as  $\epsilon$  goes to zero. Therefore

$$\lim_{\epsilon \rightarrow 0} \Gamma_{\langle S | \hat{A}_{i_\epsilon}^2} = \Gamma_S. \quad (6.15)$$

The operator  $\hat{A}[\Sigma]$  does not affect the graph of  $\langle S |$ . Next, we have to compute the planar representation of  $\Gamma_{\langle S | \hat{A}[\Sigma]}$ , which is a tangle on  $R_{\langle S | \hat{A}[\Sigma]}$ , namely a tangle on  $R_S$ . By equation (6.13), this is given by a sum of terms, one for each  $i \in \{S \cap \Sigma\}$ . Consider one of these terms. By definition of the  $\hat{\mathcal{T}}$  loop operators and of the grasp operation (Section 3), this is obtained by inserting two trivalent intersections on the spin network edge  $e_i$  (inside its ribbon), connected by a new edge of color 2. This is because the circle  $\Gamma_{\alpha_{\sigma\tau}}$  has converged to a point on  $e_i$ ; in turn, this point is then expanded inside the ribbon as a degenerate loop following back and forward a segment connecting the two intersections. By indicating the representation of the spin network simply by means of its  $e_i$  edge, we thus have

$$\begin{aligned} \langle |^{p_e} | \hat{A}_{i_\epsilon}^2 &= \frac{1}{2} \int_{\Sigma_{i_\epsilon} \otimes \Sigma_{i_\epsilon}} d^2\sigma d^2\tau \, n_a(\sigma) n_b(\tau) \langle |^{p_e} | \hat{\mathcal{T}}^{ab}[\alpha_{\sigma\tau}](\sigma, \tau) \\ &= -\frac{l_0^4}{2} \int_{\Sigma_{i_\epsilon} \otimes \Sigma_{i_\epsilon}} d^2\sigma d^2\tau \, n_a(\sigma) \Delta^a[\beta_e, \sigma] n_b(\tau) \Delta^b[\beta_e, \tau] \, p_e^2 \left\langle \begin{array}{c} p_e \\ p_e \\ p_e \end{array} \right\rangle^2, \end{aligned} \quad (6.16)$$

where we have already taken the limit (inside the integral) in the state enclosed in the brackets  $\langle |$ . Notice that this does not depend on the integration variables anymore, because the loop it contains does not represent the grasped loop for a finite  $\epsilon$ , but the a ribbon expansion of the limit state. Notice also that the two integrals are independent, and equal. Thus, we can write

$$\langle |^{p_e} | \hat{A}_{i_\epsilon}^2 = -\frac{l_0^4}{2} \left( \int_{\Sigma_{i_\epsilon}} d^2\sigma \, n_a(\sigma) \Delta^a[\beta_e, \sigma] \right)^2 p_e^2 \left\langle \begin{array}{c} p_e \\ p_e \\ p_e \end{array} \right\rangle^2 \quad (6.17)$$

The parenthesis is easy to compute. Using (2.21), it becomes the analytic form of the intersection number between the edge and the surface

$$\int_{\Sigma_{i_\epsilon}} d^2\sigma \, n_a(\sigma) \Delta^a[\beta_e, \sigma] = \int_{\Sigma_{i_\epsilon}} d^2\sigma \, n_a(\sigma) \int_{\beta_e} d\tau \, \dot{\beta}_e^a(\tau) \delta^3[\beta_e(\tau), s] = \pm 1, \quad (6.18)$$

where the sign, which depends on the relative orientation of the loop and the surface, becomes then irrelevant because of the square. Thus

$$\langle |^{p_e} | \hat{A}_i^2 = -\frac{l_0^4}{2} p_e^2 \left\langle \begin{array}{c} p_e \\ p_e \\ p_e \end{array} \right\rangle^2, \quad (6.19)$$

where we have trivially taken the limit (6.14), since there is no residual dependence on  $\epsilon$ . We have now to express the tangle inside the bracket in terms of (an edge of) a spin network state. But tangles inside ribbons satisfy recoupling theory, and we can therefore use the formula (E8) in the appendix, obtaining

$$\langle |^{p_e} | \hat{A}_{i_\epsilon}^2 = -l_0^4 p_e^2 \frac{\theta(p_e, p_e, 2)}{2\Delta_{p_e}} \langle |^{p_e} | = l_0^4 \frac{p_e(p_e + 2)}{4} \langle |^{p_e} | = l_0^4 \frac{p_e}{2} \left( \frac{p_e}{2} + 1 \right) \langle |^{p_e} |.$$

The square root in (6.13) is now easy to take because the operator  $\hat{A}_i^2$  is diagonal.

$$\langle |^{p_e} | \hat{A}_i = \langle |^{p_e} | \sqrt{\hat{A}_i^2} = \sqrt{l_0^4 \frac{p_e}{2} \left( \frac{p_e}{2} + 1 \right)} \langle |^{p_e} |. \quad (6.20)$$

Inserting in the sum (6.13), and shifting from color to spin notation, we obtain the final result

$$\langle S | \hat{A}[\Sigma] = \left( l_0^2 \sum_{i \in \{S \cap \Sigma\}} \sqrt{j_i(j_i + 1)} \right) \langle S | \quad (6.21)$$

where  $j_i$  is the spin of the edge crossing  $\Sigma$  in  $i$ . This result shows that the spin network states (with a finite number of intersection points with the surface and no vertices on the surface) are eigenstates of the area operator. The corresponding spectrum is labeled by multiplets  $\vec{j} = (j_1, \dots, j_n)$  of positive half integers, with arbitrary  $n$ , and given by

$$A_{\vec{j}}[\Sigma] = l_0^2 \sum_i \sqrt{j_i(j_i + 1)}. \quad (6.22)$$

The spectral values of the degenerate cases in which  $\Gamma_S \cap \Sigma$  includes vertices or a continuous number of points, and a discussion on the relevance of these cases, will be given elsewhere.

## VII. THE VOLUME OPERATOR

### A. The volume in terms of loop variables

Consider a three dimensional region  $\mathcal{R}$ . The volume of  $\mathcal{R}$  is given by

$$\begin{aligned} V[\mathcal{R}] &= \int_{\mathcal{R}} d^3x \sqrt{\det g} \\ &= \int_{\mathcal{R}} d^3x \sqrt{\frac{1}{3!} \left| \epsilon_{abc} \epsilon_{ijk} \tilde{E}^{ai} \tilde{E}^{bj} \tilde{E}^{ck} \right|}, \end{aligned} \quad (7.1)$$

In order to construct a regularized form of this expression, consider the three index (three hands) loop variable:

$$\mathcal{T}^{abc}[\alpha](s, t, r) = -\text{Tr}[\tilde{E}^a(s)U_\alpha(s, t) \tilde{E}^b(t)U_\alpha(t, r)\tilde{E}^c(r)U_\alpha(r, s)]. \quad (7.2)$$

Because of (A2), in the limit of the loop  $[\alpha]$  shrinking to a point  $x$  we have:

$$\mathcal{T}^{abc}[\alpha](s, t, r) \rightarrow 2\epsilon_{ijk} \tilde{E}^{ai} \tilde{E}^{bj} \tilde{E}^{ck} = 2 \epsilon^{abc} \det(\tilde{E}). \quad (7.3)$$

Following [14], fix an arbitrary chart of  $M$ , and consider a small cubic region  $\mathcal{R}_I$  of coordinate volume  $\epsilon^3$ . Let  $x_I$  be an arbitrary but fixed point in  $\mathcal{R}_I$ . Since classical fields are smooth we have  $\tilde{E}(s) = \tilde{E}(x_I) + O(\epsilon)$  for every  $s \in \mathcal{R}_I$ , and  $U_\alpha(s, t)_A^B = \mathbb{1}_A^B + O(\epsilon)$  for any  $s, t \in \mathcal{R}_I$  and straight segment  $\alpha$  joining  $s$  and  $t$ . Consider the quantity

$$W_I = \frac{1}{16 \cdot 3! \epsilon^6} \int_{\partial \mathcal{R}_I} d^2\sigma \int_{\partial \mathcal{R}_I} d^2\tau \int_{\partial \mathcal{R}_I} d^2\rho \cdot \left| n_a(\sigma) n_b(\tau) n_c(\rho) \mathcal{T}^{abc}[\alpha_{\sigma\tau\rho}](\sigma, \tau, \rho) \right|, \quad (7.4)$$

where  $\alpha_{\sigma\tau\rho}$  is a triangular loop joining the points  $\sigma$ ,  $\tau$  and  $\rho$ . Because of (7.3), we have, to lowest order in  $\epsilon$

$$\begin{aligned} W_I &= \frac{1}{8 \cdot 3! \epsilon^6} |\det(\tilde{E}(x_I))| \int_{\partial \mathcal{R}_I} d^2\sigma \int_{\partial \mathcal{R}_I} d^2\tau \int_{\partial \mathcal{R}_I} d^2\rho \cdot \\ &\quad \cdot |n_a(\sigma) n_b(\tau) n_c(\rho) \epsilon^{abc}| \\ &= |\det \tilde{E}(x_I)|, \end{aligned} \quad (7.5)$$

Thus,  $W_I$  is a non-local quantity that approximates  $\det g(x_I)$  for small  $\epsilon$ . Using the Riemann theorem as in the case of the area, we can then write the volume  $V[\mathcal{R}]$  of the region  $\mathcal{R}$  as follows. For every  $\epsilon$ , we partition of  $\mathcal{R}$  in cubes  $\mathcal{R}_{I_\epsilon}$  of coordinate volume  $\epsilon^3$ . Then

$$V[\mathcal{R}] = \lim_{\epsilon \rightarrow 0} V_\epsilon[\mathcal{R}]; \quad (7.6)$$

$$V_\epsilon[\mathcal{R}] = \sum_{I_\epsilon} \epsilon^3 W_{I_\epsilon}^{1/2}. \quad (7.7)$$

## B. Quantum volume operator

We have then immediately a definition of the quantum volume operator [14]

$$\hat{V}[\mathcal{R}] = \lim_{\epsilon \rightarrow 0} \hat{V}_\epsilon[\mathcal{R}]; \quad (7.8)$$

$$\hat{V}_\epsilon[\mathcal{R}] = \sum_{I_\epsilon} \epsilon^3 \hat{W}_{I_\epsilon}^{1/2}; \quad (7.9)$$

$$\hat{W}_{I_\epsilon} = \frac{1}{16 \cdot 3! \epsilon^6} \int_{\partial \mathcal{R}_I} d^2 \sigma \int_{\partial \mathcal{R}_I} d^2 \tau \int_{\partial \mathcal{R}_I} d^2 \rho \cdot |n_a(\sigma) n_b(\tau) n_c(\rho) \hat{\mathcal{T}}^{abc}[\alpha_{\sigma\tau\rho}](\sigma, \tau, \rho)|. \quad (7.10)$$

Notice the crucial cancellation of the  $\epsilon^6$  factor. We refer to the previous section on the area operator for the discussion on the meaning of the limit and the split of the action of the operator in the computation of the graph and the representation. We will discuss the meaning of the square root later.

Let us now begin to compute the action of this operator on a spin network state. The three surface integrals on the surface of the cube and the line integrals along the loops combine – as in the case of the area – to give three intersection numbers, which select three intersection points between the spin network and the boundary of the cube. In these three points, which we denote as  $r$ ,  $s$  and  $t$ , the loop  $\alpha_{\sigma\tau\rho}$  of the operator grasps the spin network.

Notice that the integration domain of the (three) surface integrals is a six dimensional space – the space of the possible positions of three points on the surface of a cube. Let us denote this integration domain as  $D^6$ . The absolute value in (7.10) plays a crucial role here: contributions from different points of  $D^6$  have to be taken in their absolute value, while contributions from the same point of  $D^6$  have to be summed algebraically before taking the absolute value. The position of each hand of the operator is integrated over the surface, and therefore each hand grasps each of the three points  $r$ ,  $s$  and  $t$ , producing  $3^3$  distinct terms. However, because of the absolute value, a term in which two hands grasp the same point, say  $r$ , vanishes. This happens because the result of the grasp is symmetric, but the operator is antisymmetric, in the two hands – as follows from the antisymmetry of the trace of three sigma matrices. Thus, only terms in which each hand grasps a distinct point give non vanishing contributions. For each triple of points of intersection between spin network and cube's surface  $r$ ,  $s$  and  $t$ , there are  $3!$  ways in which the three hands can grasp the three points. These  $3!$  terms have alternating signs because of the antisymmetry of the operator, but the absolute value prevents the sum from vanishing, and yields the same contribution for each of the  $3!$  terms.

If there are only two intersection points between the boundary of the cube and the spin network, then there are always two hands grasping in the same point; contributions have to be summed before taking the absolute value, and thus they cancel. Thus, the sum in (7.9) reduces to a sum over the cubes  $I_\epsilon^i$  whose boundary has at least three distinct intersections with the spin network, and the surface integration reduces to a sum over the triple-grasplings in *distinct* points. For  $\epsilon$  small enough, the only cubes whose surface has at least three intersections with the spin network are the cubes containing a vertex  $i$  of the spin network. Therefore, the sum over cubes reduces to a sum over the vertices  $i \in \{S \cap \mathcal{R}\}$  of the spin network, contained inside  $\mathcal{R}$ . Let us denote by  $I_{i_\epsilon}$  the cube containing the vertex  $i$ . We then have

$$\begin{aligned} \langle S | \hat{V}[\mathcal{R}] &= \lim_{\epsilon \rightarrow 0} \sum_{i \in \{S \cap \mathcal{V}\}} \epsilon^3 \langle S | \sqrt{|\hat{W}_{I_\epsilon^i}|} \\ \langle S | \hat{W}_{I_\epsilon^i} &= \frac{i l_0^6}{16 \cdot 3! \epsilon^6} \sum_{s,t,r} \left\langle S \#_{s,t,r} \alpha_{s,t,r} \right|, \end{aligned} \quad (7.11)$$

where  $s$ ,  $t$  and  $r$  are three *distinct* intersections between the spin network and the boundary of the box, and we have indicated by  $\left\langle S \#_{s,t,r} \alpha_{s,t,r} \right|$  the result of the triple grasp of the three hands operator with loop  $\alpha_{str}$  on  $S$ .

Let us compute one of the terms above, corresponding to a given triple of grasps, over an  $n$ -valent intersections. First of all, in the limit  $\epsilon \rightarrow 0$  the operator does not change the graph of the quantum state, for the same reason the area operator doesn't. Thus, the computation reduces to a combinatorial computation of the action of the operator on the representation of the planar state, involving recoupling theory.

Let us represent a spin network state simply by means of the portion of its virtual net containing the vertex on which the operator is acting. We have

$$\left\langle \begin{array}{c} P_2 \quad \dots \quad P_{n-3} \\ \diagdown \quad \diagup \quad \diagdown \quad \diagup \\ \bullet \quad \dots \quad \bullet \\ \diagup \quad \diagdown \quad \diagup \quad \diagdown \\ P_1 \quad i_2 \quad i_3 \quad \dots \quad i_{n-2} \quad P_{n-2} \\ \diagdown \quad \diagup \quad \diagdown \quad \diagup \\ P_0 \quad i_1 \quad i_{n-1} \quad P_{n-1} \end{array} \right| \hat{W}_{I_\epsilon^i} = \quad (7.12)$$



$$= \frac{i!_0^6}{16 \, 3!} \sum_{\substack{r=0, \dots, n-1 \\ t=0, \dots, n-1 \\ s=0, \dots, n-1}} \int_{\partial \mathcal{V}_I \otimes \partial \mathcal{V}_I \otimes \partial \mathcal{V}_I} d^2 \sigma d^2 \tau d^2 \rho \left| n_a(\sigma) \Delta^a[\gamma, \sigma] \, n_b(\tau) \Delta^b[\gamma, \tau] \, n_c(\rho) \Delta^c[\gamma, \rho] \right|$$

where  $W_{[rts]}^{(n)}$  is the operator that grasp the  $r$ ,  $t$  and  $s$  edge of the the  $n$ -valent vertex as follow:

[illegible]

Notice that we have replaced the triangular loop with vertices  $r$ ,  $s$  and  $t$  by three edges of color 2 joining the three points  $r$ ,  $s$  and  $t$  to a trivalent vertex. This can be done as follows. First we deform the triangle over the ribbon-net. Indeed, as remarked for the case of the area, the tangle above does not represent a tangle extended in  $M$ , but just the expansion over the ribbon net of a rooting of lines in a single point of  $M$ . Second, we notice that we can antisymmetrize the two lines that exit from the hand of an operator by using the binor identity, because tracing a hand with a zero length loop gives a vanishing quantity.

The last equality in the last equation follows from the fact that trivalent spin network form a basis (see Sec. V). From eq. (7.12) we see that the action of  $\hat{W}_{I_i}$  splits into a multiplication by a numerical prefactor and a recoupling part given by eq. (7.13), which does not depend on the integration variables. Using eq. (6.18) we can perform the integration in eq. (7.12). This yields the intersection number between the edges  $r$ ,  $s$  and  $t$  and the surface of the cube  $\mathcal{V}_I$ . The sign of the intersection number, coming from the relative orientation of the loop and the surface, is irrelevant, because of the presence of the absolute value.

Because of the symmetry properties of the 3-valent node (222), the  $3!$  terms in eq. (7.13) are related by:

$$\hat{W}_{[i_1 i_2 i_3]}^{(n)} = (-1)^p \hat{W}_{[i_{p1} i_{p2} i_{p3}]}^{(n)} \quad (7.14)$$

where  $p_i$  it is a permutation of 123, and  $p$  it is the order of the permutation. Thus, the action the volume operator on a generic spin network state  $\langle S|$  is given by:

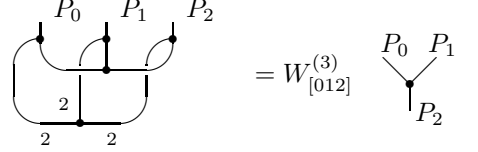
$$\hat{V}[\nu] = l_0^3 \sum_{i \in \{\text{Sn}\nu\}} \sqrt{\sum_{\substack{r=0, \dots, n-3 \\ t=r+1, \dots, n-2 \\ s=t+1, \dots, n-1}} \left| \frac{i}{16} \hat{W}_{[rts]}^{(n_i)} \right|} \quad (7.15)$$

where  $n_i$  is the valence of the  $i$ -th intersection. Equations (7.13) and (7.15) completely define the volume operator. There are two remaining tasks: to find the explicit expression for the matrix  $iW_{[rst]k_1 \dots i_3 k_2}^{(n)}(P_{n-1}, \dots, P_0)$ , which is

defined in eq. (7.13) only implicitly; and to show that the absolute value and the square root in equation (7.15) are well defined. Below, we complete both tasks: we provide an explicit expression for  $iW_{[rst]k_{n-2}\dots k_3k_2}^{(n) i_{n-2}\dots i_3i_2}(P_{n-1}, \dots, P_0)$ , and we prove that the argument of the absolute value is a diagonalizable finite dimensional matrix with real eigenvalues, and the argument of the square root is a finite dimensional diagonalizable matrix with positive real eigenvalues.

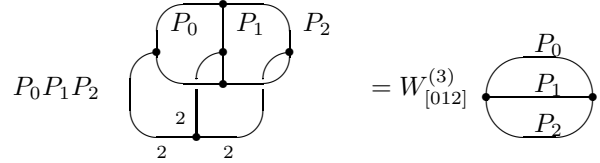
### C. Trivalent vertices

We begin studying the case  $n = 3$ . It is easy to see that  $W_{[012]}^{(3)} = 0$  from the relation



$$= W_{[012]}^{(3)} \begin{array}{c} P_0 \quad P_1 \\ \diagdown \quad \diagup \\ \bullet \\ \diagup \quad \diagdown \\ P_2 \end{array} . \quad (7.16)$$

In fact, by closing the generic 3-valent node with itself we have



$$P_0 P_1 P_2 \begin{array}{c} P_0 \quad P_1 \quad P_2 \\ \diagdown \quad \diagup \quad \diagup \\ \bullet \\ \diagup \quad \diagdown \quad \diagdown \\ 2 \quad 2 \end{array} = W_{[012]}^{(3)} \begin{array}{c} P_0 \\ \diagdown \quad \diagup \\ \bullet \\ \diagup \quad \diagdown \\ P_1 \quad P_2 \end{array} . \quad (7.17)$$

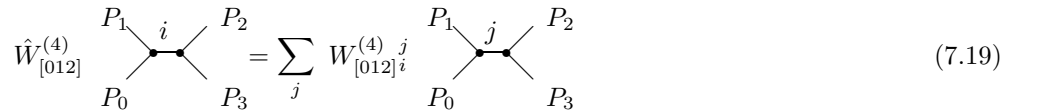
Thus  $W_{[012]}^{(3)}$  is determined by the Wigner 9J-symbol (the evaluation of the hexagonal net) as:

$$W_{[012]}^{(3)} = \frac{P_0 P_1 P_2 \left\{ \begin{array}{ccc} P_0 & P_1 & P_2 \\ P_0 & P_1 & P_2 \\ 2 & 2 & 2 \end{array} \right\}}{\theta(P_0, P_1, P_2)} . \quad (7.18)$$

But the hexagonal net (in the case of  $A = \pm 1$ ) it is antisymmetric for the exchange of two columns or of two rows. Therefore the matrix  $W^3$  vanishes, and the trivalent vertices give no contribution to the volume. We have re-derived the result that the volume of a 3-valent vertex is zero, first obtained by Loll [15].

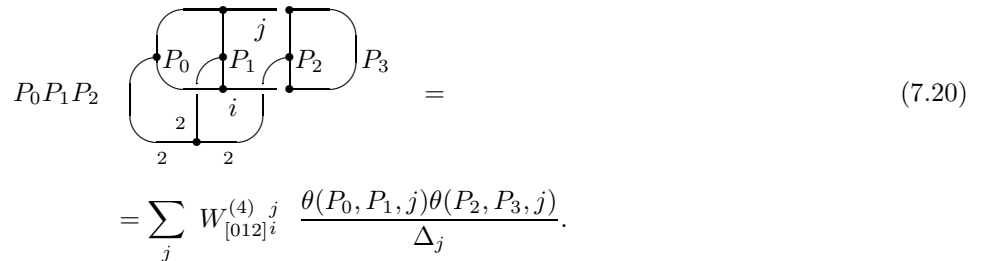
### D. Four-valent vertices

Next, we study the  $n = 4$  case.



$$\hat{W}_{[012]}^{(4)} \begin{array}{c} P_1 \quad i \quad P_2 \\ \diagdown \quad \diagup \quad \diagup \\ \bullet \\ \diagup \quad \diagdown \quad \diagdown \\ P_0 \quad P_3 \end{array} = \sum_j W_{[012]i}^{(4) j} \begin{array}{c} P_1 \quad j \quad P_2 \\ \diagdown \quad \diagup \quad \diagup \\ \bullet \\ \diagup \quad \diagdown \quad \diagdown \\ P_0 \quad P_3 \end{array} \quad (7.19)$$

Using the same technique of the 3-valent node we can compute the matrix  $W_{[012]i}^{(4) j}$  for a 4-valent node as follows



$$P_0 P_1 P_2 \begin{array}{c} P_0 \quad P_1 \quad P_2 \quad P_3 \\ \diagdown \quad \diagup \quad \diagup \quad \diagup \\ \bullet \\ \diagup \quad \diagdown \quad \diagdown \quad \diagdown \\ 2 \quad i \quad 2 \end{array} = \sum_j W_{[012]i}^{(4) j} \frac{\theta(P_0, P_1, j) \theta(P_2, P_3, j)}{\Delta_j} . \quad (7.20)$$

Using the relation

$$\begin{array}{c} \text{2} \quad \quad j \\ \diagdown \quad \diagup \\ \bullet \quad \bullet \\ \diagup \quad \diagdown \\ P_2 \quad P_3 \\ | \\ i \end{array} = \frac{Tet \begin{bmatrix} i & j & P_3 \\ P_2 & P_2 & 2 \end{bmatrix}}{\theta(2, j, i)} \begin{array}{c} \text{2} \quad j \\ \diagdown \quad \diagup \\ \bullet \\ | \\ i \end{array}, \quad (7.21)$$

we obtain:

$$\begin{aligned} W_{[012]i}^{(4)j} &= \frac{P_0 P_1 P_2 \left\{ \begin{array}{ccc} P_0 & P_1 & j \\ P_0 & P_1 & i \\ 2 & 2 & 2 \end{array} \right\} Tet \begin{bmatrix} i & j & P_3 \\ P_2 & P_2 & 2 \end{bmatrix}}{\theta(2, j, i)} \cdot \frac{\Delta_j}{\theta(P_0, P_1, j) \theta(P_2, P_3, j)}. \end{aligned} \quad (7.22)$$

We now prove that the matrix  $i \cdot W_{[012]i}^{(4)j}$  is diagonalizable with real eigenvalues and, as a consequence, that its absolute values is well defined. To this aim, let us define the notation:

$$A_i^j = \frac{P_0 P_1 P_2 \left\{ \begin{array}{ccc} P_0 & P_1 & j \\ P_0 & P_1 & i \\ 2 & 2 & 2 \end{array} \right\} Tet \begin{bmatrix} i & j & P_3 \\ P_2 & P_2 & 2 \end{bmatrix}}{\theta(2, j, i)} \quad (7.23)$$

$$M(i) = \sqrt{\frac{\Delta_i}{\theta(P_0, P_1, i) \theta(P_2, P_3, i)}} \quad (7.24)$$

$$\tilde{W}_i^j = M(i) M(j) A_i^j \quad (7.25)$$

$$S_i^j = \delta_i^j M(i). \quad (7.26)$$

The matrix  $S_i^j$  can be consider as a change of basis in the space of the 4-valent vertices and the matrix  $i \cdot W_{[012]i}^{(4)j}$  can be rewritten as:

$$i W_{[012]i}^{(4)j} = (S^{-1})_i^k \cdot (i \tilde{W}_k^l) \cdot S_l^j, \quad (7.27)$$

where, because of the antisymmetry properties of the 9J-symbol under exchange of two rows and the symmetry property of the *Tet* symbol<sup>7</sup>, the matrix  $\tilde{W}_k^l$  is antisymmetric. We have shown that in the basis

$$\mathbf{n}_i = \sqrt{\frac{\begin{array}{c} \text{---} \text{---} \text{---} \\ \text{---} \text{---} \text{---} \\ \text{---} \text{---} \end{array}}{\begin{array}{c} \text{---} \text{---} \text{---} \\ \text{---} \text{---} \text{---} \\ \text{---} \text{---} \end{array}}} \begin{array}{c} P_1 \quad \quad P_2 \\ \diagdown \quad \diagup \\ \bullet \\ \diagup \quad \diagdown \\ P_0 \quad \quad P_3 \end{array} \quad (7.28)$$

the action, eq. (7.19), of the operator  $\hat{W}_{[012]}^{(4)}$  is given by:

$$\hat{W}_{[012]}^{(4)} \mathbf{n}_i = \sum_j \tilde{W}_{[012]i}^{(4)j} \mathbf{n}_j \quad (7.29)$$

where  $\tilde{W}_{[012]i}^{(4)j}$  a *real antisymmetric* matrix. Moreover, from the admissibility condition for the 3-valent node of eq. (7.21), we see that  $\tilde{W}_k^l$  vanishes unless  $k = l$  or  $k = l \pm 2$ . Thus, we have show that the operator  $i \hat{W}_{[012]}^{(4)}$  may be represented by a purely imaginary antisymmetric matrix  $i \tilde{W}_k^l$  with non-vanishing matrix elements only for  $k = l \pm 2$ . Such matrix is diagonalizable and has real eigenvalues.

---

<sup>7</sup>For a discussion of the symmetry properties of the 9J-symbol and related quantities, see for instance [39]

Furthermore, notice the following. We write the dependence on the coloring of the external edges explicitly; namely we write  $W_{[012]i}^{(4)j}(P_0, P_1, P_2, P_3)$ . Using eq. (7.20), it is easy to see that the following relations hold between the matrices  $W_{[i_1 i_2 i_3]i}^{(4)j}(P_0, P_1, P_2, P_3)$

$$\begin{aligned} W_{[013]i}^{(4)j}(P_0, P_1, P_2, P_3) &= W_{[012]i}^{(4)j}(P_0, P_1, P_3, P_2), \\ W_{[023]i}^{(4)j}(P_0, P_1, P_2, P_3) &= -W_{[123]i}^{(4)j}(P_3, P_2, P_1, P_0), \\ W_{[123]i}^{(4)j}(P_0, P_1, P_2, P_3) &= -W_{[012]i}^{(4)j}(P_3, P_2, P_0, P_1). \end{aligned} \quad (7.30)$$

We have shown that there exists a basis  $\mathbf{n}_i$  in which the four operators  $i\hat{W}_{[i_1 i_2 i_3]}^{(4)}$  that define the action of the volume on four valent vertices, are purely imaginary antisymmetric matrices. The eigenvalues of the four operators  $i\hat{W}_{[i_1 i_2 i_3]}^{(4)}$  are real and, if  $x$  is an eigenvalue, so is  $-x$ . Therefore, the absolute value of the matrices  $i\hat{W}_{[i_1 i_2 i_3]}^{(4)}$  is well defined. It is given by a non-negative (i.e., having real eigenvalues equal or greater than zero) antisymmetric matrix. But the sum of non-negative matrices is a non-negative matrix. Therefore the sum of the the absolute values of the four matrices  $i\hat{W}_{[i_1 i_2 i_3]}^{(4)}$  is a non-negative antisymmetric matrix as well. Thus, the volume operator is diagonalizable on the spin network basis, *with positive real eigenvalues*, if all the vertices have valence 3, 4. Below, we show that these results extend to vertices of arbitrary valence.

### E. The case of an $n$ -vertex

We now shown that there exists a basis in which all the operators  $i\hat{W}_{[i_1 i_2 i_3]}^{(n)}(P_0, \dots, P_{n-1})$  are represented by a purely imaginary antisymmetric matrix. Consider eq. (7.13). By repeated application of the recoupling theorem, eq. (7.13) can be rewritten as

$$P_r P_t P_s \left( \begin{array}{c} P_0 \quad P_r \quad P_t \quad P_s \quad \dots \quad P_{n-1} \\ \text{Diagram with arcs and labels } \hat{i}_2, \hat{i}_3, \hat{i}_4, \dots \end{array} \right) = W_{[rst]\hat{i}_2 \dots \hat{i}_{n-2}}^{(n) \hat{k}_2 \dots \hat{k}_{n-2}} \cdot \left( \begin{array}{c} P_0 \quad P_r \quad P_t \quad P_s \quad \dots \quad P_{n-1} \\ \text{Diagram with arcs and labels } \hat{k}_2, \hat{k}_3, \hat{k}_4, \dots \end{array} \right) \quad (7.31)$$

(we have assumed, without loss of generality, that there is no grasp on the  $P_0$  or  $P_{n-1}$  edge). Closing the vertex with itself and using the relation (E8) and (E9), we find

$$W_{[rst]\hat{i}_2 \dots \hat{i}_{n-2}}^{(n) \hat{k}_2 \dots \hat{k}_{n-2}} = P_r P_t P_s \left\{ \begin{array}{ccc} \hat{k}_2 & P_t & \hat{k}_3 \\ \hat{i}_2 & P_t & \hat{i}_3 \\ 2 & 2 & 2 \end{array} \right\} \cdot \frac{-1 \lambda_{\hat{k}_2}^{\hat{i}_2} \delta_{\hat{i}_4}^{\hat{k}_4} \dots \delta_{\hat{i}_{n-2}}^{\hat{k}_{n-2}} \cdot Tet \left[ \begin{array}{ccc} P_r & P_r & P_0 \\ \hat{k}_2 & \hat{i}_2 & 2 \end{array} \right] Tet \left[ \begin{array}{ccc} \hat{i}_3 & \hat{k}_3 & \hat{k}_4 \\ P_s & P_s & 2 \end{array} \right] \Delta_{\hat{k}_2} \Delta_{\hat{k}_3}}{\theta(\hat{k}_2, 2, \hat{i}_2) \theta(\hat{k}_3, 2, \hat{i}_3) \theta(P_0, P_r, \hat{k}_2) \theta(\hat{k}_2, P_t, \hat{k}_3) \theta(\hat{k}_3, P_s, \hat{k}_4)} \quad (7.32)$$

We now change basis in the same fashion as we did for the 4-valent vertex, [see Eq. (7.28)]. We define a new basis in which any edge (real or virtual) is multiplied by  $\sqrt{\Delta_i}$  ( $i$  coloring of the edge) and any vertex is divided by  $\sqrt{\theta(a, b, c)}$  ( $a, b$  and  $c$  the coloring of the edges adjacent to the vertex). It is then easy to see that in this new basis the matrix on eq. (7.32) becomes real antisymmetric. Indeed, we have simply reduced the general problem to the case of four valent vertices. Now, the key result, that we shall prove in the next section is that, in the basis we have defined, the recoupling theorem is a *unitary* transformation. A unitary transformation preserves the property of a matrix of being diagonalizable and having real eigenvalues. It follows that the results we have obtained for the four-valent vertices hold in general.

We are now ready to find an explicit expression for the recoupling matrix  $iW_{[rst]k_{n-2} \dots k_3 k_2}^{(n) i_{n-2} \dots i_3 i_2}(P_{n-1}, \dots, P_0)$  of eq. (7.13) for a general valence  $n$  of the vertex. Let us begin by sketching the procedure that we follow. First, the recoupling theorem allows us to move one of the three grasps from the external edge, say  $P_r$ , of eq. (7.13), and bring it to a virtual vertex. We denote this operation as Move 1:

$$\frac{\text{Diagram with } P_r \text{ and } i_r \text{ on a vertex}}{2} = \sum_{k_r} \left\{ \begin{array}{ccc} i_{r+1} & i_r & k_r \\ 2 & P_r & P_r \end{array} \right\} \frac{\text{Diagram with } P_r \text{ and } i_r \text{ on a vertex}}{2} \quad (7.33)$$

$$= \sum_{k_r} \left\{ \begin{matrix} i_{r+1} & i_r & k_r \\ 2 & P_r & P_r \end{matrix} \right\} [\lambda_{k_r}^{2i_r}]^{-1} \begin{array}{c} P_r \\ | \\ \bullet \\ i_r \quad i_{r+1} \\ | \quad | \\ 2 \end{array} .$$

Second, we can use recoupling theorem repeatedly to move the grasp all the way to the edge  $P_0$ . We denote this operation as Move 2:

$$\begin{array}{c} P_{r-1} \\ | \\ \bullet \\ i_r \quad k_r \\ | \quad | \\ i_{r-1} \quad 2 \end{array} = \sum_{k_r} \left\{ \begin{matrix} k_r & 2 & k_{r-1} \\ i_{r-1} & P_{r-1} & i_r \end{matrix} \right\} \begin{array}{c} P_{r-1} \\ | \\ \bullet \\ i_{r-1} \quad k_r \\ | \quad | \\ k_{r-1} \quad 2 \end{array} . \quad (7.34)$$

In this way we can bring all three grasps to the edge  $P_0$ . The final step is just given by recognizing that we have Tet structure on the edge  $P_0$ .

Let us begin by applying Move 1 to the node  $r$ . We obtain

$$\left\langle \begin{array}{c} P_1 \\ | \\ \bullet \\ i_1 \\ | \\ P_0 \end{array} \begin{array}{c} P_{r-1} \\ | \\ \bullet \\ i_{r-1} \\ | \\ 2 \end{array} \begin{array}{c} P_r \\ | \\ \bullet \\ i_r \\ | \\ 2 \end{array} \begin{array}{c} P_t \\ | \\ \bullet \\ i_t \\ | \\ 2 \end{array} \begin{array}{c} P_s \\ | \\ \bullet \\ i_s \\ | \\ P_{n-1} \end{array} \right\rangle \quad (7.35)$$

Then, using Move 2 we can move the  $(i_r, k_r, 2)$  node to the left of the node  $(i_{r-1}, P_{r-1}, i_t)$ :

$$\left\langle \begin{array}{c} P_1 \\ | \\ \bullet \\ i_1 \\ | \\ P_0 \end{array} \begin{array}{c} P_{r-1} \\ | \\ \bullet \\ i_{r-1} \\ | \\ 2 \end{array} \begin{array}{c} P_r \\ | \\ \bullet \\ k_r \\ | \\ 2 \end{array} \begin{array}{c} P_t \\ | \\ \bullet \\ i_t \\ | \\ 2 \end{array} \begin{array}{c} P_s \\ | \\ \bullet \\ i_s \\ | \\ P_{n-1} \end{array} \right\rangle \quad (7.36)$$

We repeat move 2 until the first node with the 2 edge is coupled to the  $P_0$  edge. In this way, after a finite number of moves 2, we have transformed the original network to

$$\left\langle \begin{array}{c} P_1 \\ | \\ \bullet \\ k_1 \\ | \\ P_0 \end{array} \begin{array}{c} P_r \\ | \\ \bullet \\ k_r \\ | \\ 2 \end{array} \begin{array}{c} P_t \\ | \\ \bullet \\ i_t \\ | \\ 2 \end{array} \begin{array}{c} P_s \\ | \\ \bullet \\ i_s \\ | \\ P_{n-1} \end{array} \right\rangle \quad (7.37)$$

Before repeating this procedure for each of the three grasps, it is convenient to rename the colors  $k_a$  of the virtual edges as  $\bar{k}_a$  (and to replace the remaining  $i_a$  by  $k_a$  as well; this can be done by inserting a sum over a  $\bar{k}_a$  multiplied by a  $\delta_{i_a}^{\bar{k}_a}$ ).

Repeating the sequence of moves for the two grasps over the edges  $r$  and  $s$ , we transform the grasped vertex to the following final form:

$$\left\langle \begin{array}{c} \bar{k}_1 \\ | \\ \bar{k}_1 \\ | \\ P_0 \end{array} \begin{array}{c} P_2 \\ | \\ \bullet \\ k_1 \\ | \\ 2 \end{array} \dots \begin{array}{c} P_{n-3} \\ | \\ \bullet \\ k_{n-2} \\ | \\ 2 \end{array} \begin{array}{c} P_{n-2} \\ | \\ \bullet \\ k_{n-1} \\ | \\ P_{n-1} \end{array} \right\rangle . \quad (7.38)$$

This is equal to the original  $n$ -valent vertex with the  $i_a$  replaced by  $k_a$  and multiplied by  $Tet[k_1, \bar{k}_1, \bar{k}_1; 2, 2, 2]$  (see eq. (E9)). Bringing all together, we have shown that the action of the volume operator is described by the sum (7.15) extended over all vertices of the spin network, where the explicit form for the recoupling matrix (7.13) is given by

$$\begin{aligned}
W_{[rst]i_2 \dots i_{n-2}}^{(n) k_2 \dots k_{n-2}}(P_0, \dots, P_{n-1}) = & \sum_{\bar{k}_1, \dots, \bar{k}_{n-2}} \sum_{\tilde{k}_1, \dots, \tilde{k}_{n-2}} P_t P_r P_s \cdot \frac{Tet \left[ \begin{smallmatrix} \bar{k}_1 & \tilde{k}_1 & k_1 \\ 2 & 2 & 2 \end{smallmatrix} \right]}{\Delta_{P_0}} \\
& \cdot \left[ \prod_{a=r+1}^{n-2} \delta_{i_a}^{\bar{k}_a} \right] \cdot M \left[ \begin{smallmatrix} i_{r+1} & i_r & \bar{k}_r \\ 2 & r & P_r \end{smallmatrix} \right] \cdot \left[ \prod_{a=1}^{r-1} \left\{ \begin{smallmatrix} \bar{k}_{a+1} & 2 & \bar{k}_a \\ i_a & P_a & i_{a+1} \end{smallmatrix} \right\} \right] \\
& \cdot \left[ \prod_{b=t+1}^{n-2} \delta_{i_b}^{\tilde{k}_b} \right] \cdot M \left[ \begin{smallmatrix} \bar{k}_{r+1} & \bar{k}_r & \tilde{k}_r \\ 2 & t & P_t \end{smallmatrix} \right] \cdot \left[ \prod_{b=1}^{t-1} \left\{ \begin{smallmatrix} \tilde{k}_{b+1} & 2 & \tilde{k}_b \\ \bar{k}_b & P_a & \bar{k}_{b+1} \end{smallmatrix} \right\} \right] \\
& \cdot \left[ \prod_{c=s+1}^{n-2} \delta_{i_c}^{k_c} \right] \cdot M \left[ \begin{smallmatrix} \tilde{k}_{s+1} & \tilde{k}_s & k_s \\ 2 & s & P_s \end{smallmatrix} \right] \cdot \left[ \prod_{c=1}^{s-1} \left\{ \begin{smallmatrix} k_{c+1} & 2 & k_c \\ \tilde{k}_c & P_a & \tilde{k}_{c+1} \end{smallmatrix} \right\} \right]
\end{aligned} \tag{7.39}$$

and

$$M \left[ \begin{smallmatrix} i_{r+1} & i_r & k_r \\ 2 & r & P_r \end{smallmatrix} \right] = \begin{cases} 1, & r = 0; \\ [\lambda_{k_r}^{2i_r}]^{-1} \left\{ \begin{smallmatrix} i_{r+1} & i_r & k_r \\ 2 & P_r & P_r \end{smallmatrix} \right\}, & 0 < r < n-1; \\ \lambda_{P_{n-1}}^{2P_{n-1}} = -1, & r = n-1. \end{cases} \tag{7.40}$$

where  $i_1 = k_1 = P_0$  and  $i_{n-1} = k_{n-1} = \bar{k}_{n-1} = \tilde{k}_{n-1} = P_{-1}$ . (We have used the fact that for  $A = -1$ ,  $\lambda_a^{2a} = -1$ .)

This formula can be specialized to the case of three-vertex ( $n = 3$ ) and four-vertex ( $n = 4$ ). In the case of three-vertex we have:

$$W^{(3)}(P_0, P_1, P_2) = \left| \sum_{\tilde{k}_1} P_0 P_1 P_2 [\lambda_{P_0}^{2\tilde{k}_1}]^{-1} \left\{ \begin{smallmatrix} P_2 & 2 & P_0 \\ \tilde{k}_1 & P_1 & P_2 \end{smallmatrix} \right\} \left\{ \begin{smallmatrix} P_2 & P_0 & \tilde{k}_1 \\ 2 & P_1 & P_1 \end{smallmatrix} \right\} \frac{Tet \left[ \begin{smallmatrix} P_0 & \tilde{k}_1 & P_0 \\ 2 & 2 & 2 \end{smallmatrix} \right]}{\Delta_{P_0}} \right|. \tag{7.41}$$

and a direct computation confirms that the volume of any three-vertex is 0. For the case of four-valent vertex, we obtain the formula:

$$W_{[013]i}^{(4) k} = \sum_{\tilde{k}_1} P_0 P_1 P_3 (-1) [\lambda_{P_0}^{2\tilde{k}_1}]^{-1} \left\{ \begin{smallmatrix} i & P_0 & \tilde{k}_1 \\ 2 & P_1 & P_1 \end{smallmatrix} \right\} \left\{ \begin{smallmatrix} P_3 & 2 & k \\ i & P_2 & P_3 \end{smallmatrix} \right\} \left\{ \begin{smallmatrix} k & 2 & P_0 \\ \tilde{k}_1 & P_1 & i \end{smallmatrix} \right\} \cdot \frac{Tet \left[ \begin{smallmatrix} P_0 & \tilde{k}_1 & P_0 \\ 2 & 2 & 2 \end{smallmatrix} \right]}{\Delta_{P_0}}$$

and the other 3 matrix that appear in the definition of the action of the volume operator are easily deduced from the identities (7.30).

## F. Summary of the volume's action

Finally, let us summarize the procedure for computing the eigenvalues and eigenvectors of the volume. Consider the spin-network states  $\langle S |$  with a fixed graph and a fixed coloring of the real edges, but with arbitrary intersections. The set of these spin networks forms a finite dimensional subspace  $V$  of the quantum state space. The subspace  $V$  is invariant under the action of the volume operator. We denote the valence of the real vertex  $i$  by  $n_i$ . Fix a trivalent decomposition of each vertex  $i \in \{S \cup \mathcal{R}\}$ . Consider all compatible colorings of the virtual edges. For every vertex, the number of the compatible colorings depends on the valence of the vertex, as well as on the coloring of the external edges. Let  $N_i$  be the number of compatible colorings of the vertex  $n_i$ . The dimension  $N$  of the subspace  $V$  we are considering is  $N = \prod_i N_i$ . Our aim is to diagonalize the volume operator in  $V$ .

We indicate a basis in  $V$  as follows. Given a vertex  $i$  with valence  $n_i$ , we have previously denoted compatible colorings of the internal edges by  $(i_2, \dots, i_{n_i-2})$ . It is more convenient here to simplify the notation by introducing a single index  $K_i = 1, N_i$ , which labels all compatible internal colorings of the vertex  $i$ .

We now recall the basic expression we have obtained for the volume, namely eq. (7.15):

$$\hat{V}[\mathcal{V}] = l_0^3 \sum_{i \in \{S \cap \mathcal{V}\}} \hat{V}_i,$$

$$\hat{V}_i = \sqrt{\sum_{\substack{r=0,\dots,n-3 \\ t=r+1,\dots,n-2 \\ s=t+1,\dots,n-1}} \left| \frac{i}{16} \hat{W}_{[rts]}^{(n_i)} \right|}, \quad (7.42)$$

where the first sum is over the vertices and the second sum is over the triples of edges adjacent to the vertex. We have shown that the operators  $i\hat{W}_{[rts]}^{(n_i)}$  are diagonalizable matrices with real eigenvalues. These matrices have components

$$\hat{W}_{[rts]K_{I_i}}^{(n_i)\bar{K}_{I_i}} = [\text{l.h.s. of eq. (7.39)}]. \quad (7.43)$$

Since the matrices  $i\hat{W}_{[rts]K_{I_i}}^{(n_i)\bar{K}_{I_i}}$  are diagonalizable with real eigenvalues, from the spectral theorem we can write them as:

$$i\hat{W}_{[rts]}^{(n_i)} = \sum_{\alpha} \alpha \lambda_{[rts]}^{(n_i)} \alpha \hat{P}_{[rts]}^{(i)}, \quad (7.44)$$

where  $\alpha \lambda_{[rts]}^{(n_i)}$  are real quantities and the  $\alpha \hat{P}_{[rts]}^{(i)}$  are the spectral projectors of the finite dimensional matrix operator  $\hat{W}_{[rts]}^{(n_i)}$ , acting on the  $i$ -th vertex's basis.

From (7.42), we have then

$$\hat{V}_i^2 = \sum_{\substack{r=0,\dots,n_i-3 \\ t=r+1,\dots,n_i-2 \\ s=t+1,\dots,n_i-1}} \sum_{\alpha} \frac{|\lambda_{\alpha}^{[rts]}|}{16} \alpha \hat{P}_{[rts]}^{(n_i)}. \quad (7.45)$$

Being the sum of hermitian non-negative matrices,  $\hat{V}_i^2$  as well is diagonalizable with real non-negative eigenvalues, which we denote as  $\lambda_{\beta_i}^2$ , and spectral projectors  $\hat{P}_{\beta_i}$ :

$$\hat{V}_i^2 = \sum_{\beta_i} \lambda_{\beta_i}^2 \hat{P}_{\beta_i}. \quad (7.46)$$

with  $\lambda_{\beta_i} \geq 0$ . Therefore we have

$$\hat{V}_i = \sum_{\beta_i} \lambda_{\beta_i} \hat{P}_{\beta_i} \quad (7.47)$$

and the volume is given by

$$\hat{V}[\mathcal{V}] = l_0^3 \sum_{i \in \{S \cap \mathcal{V}\}} \sum_{\beta_i} \lambda_{\beta_i} \hat{P}_{\beta_i}. \quad (7.48)$$

Now, the projectors acting on different vertices commute among themselves:  $\hat{P}_{\beta_i} \hat{P}_{\beta'_j} = \hat{P}_{\beta'_j} \hat{P}_{\beta_i}$  if  $i \neq j$ . Therefore the eigenvectors of  $\hat{V}$  are the common eigenvectors of all  $\hat{V}_i$ . They are labeled by one  $\beta_i$  for every vertex  $i$ , namely by a multi-index  $\vec{\beta} = (\beta_1 \dots \beta_p)$ , where  $p$  is the number of vertices in the region. The corresponding spectral projectors  $\hat{P}_{\vec{\beta}}$  of  $\hat{V}$  are the products over the vertices of the spectral projectors of the vertex volume operators  $\hat{V}_i$

$$\hat{P}_{\vec{\beta}} = \prod_i \hat{P}_{\beta_i}. \quad (7.49)$$

It is immediate to conclude that

$$\hat{V} = l_0^3 \sum_{\vec{\beta}} \lambda_{\vec{\beta}} \hat{P}_{\vec{\beta}}, \quad (7.50)$$

where the eigenvalues of the volume are the sums of the eigenvalues of the volume of each intersection:

$$\lambda_{\vec{\beta}} = \sum_i \lambda_{\beta_i}. \quad (7.51)$$

The problem of the determination of the spectrum of the volume is reduced to a well defined calculation of the eigenvalues  $\lambda_{\beta_i}$ , which depend on the valence and coloring of adjacent vertices of the vertex  $i$ . Let us summarize the various steps of this computation. Given an arbitrary real vertex  $i$  with coloring of adjacent edges  $P_0, \dots, P_{n_i-1}$ : **(i)** determine the set of the possible colorings of its virtual edges, and label them by an index  $K_i$ ; **(ii)** using eq. (7.39) compute the matrix elements  $\hat{W}_{[rts]K_i}^{(n_i)}$ ; **(iii)** for each of this matrices, compute its spectral decomposition, i.e. the eigenvalues  ${}^\alpha\lambda_{[rts]}^{(n_i)}$  and the spectral projectors  ${}^\alpha\hat{P}_{[rts]}^{(n_i)}$ ; **(iv)** compute the matrix  $\hat{V}_i$  from eq. (7.45); **(v)** compute the eigenvalues of the matrix  $\hat{V}_i$ . The square root of these give the  $\lambda_{\beta_i}$ 's. All these steps can be fully performed using an algebraic manipulation program such as *Mathematica*. We have written a *Mathematica* program that performs these calculations, and we will give free access to this program on line. In Appendix F we give the values of the quantities  $\lambda_{\beta_i}(P_0, \dots, P_{n_i-1})$  for some 4-valent and 5-valent vertex, computed using this program.

### VIII. THE SCALAR PRODUCT

The results above allow us to introduce a scalar product in the loop representation. The original definition of the loop representation of quantum general relativity left the problem of fixing the scalar product undetermined: the scalar product had to be determined by requiring quantum observables to be hermitian [3]. The problem was complicated by the fact that the loop “basis” is overcomplete. Later, the introduction of the non-overcomplete spin network basis, and the realization that spin network states (with suitable bases chosen on the high-valent vertices) are eigenstates of the geometry, lead to the natural suggestion that spin network states ought to be orthogonal. For no reason, however, these states ought to be *ortho-normal*; namely the norm of the spin network states remained undetermined. The methods introduced in this paper allow us to complete the process, suggest a norm for the spin network states, and thus yield a complete definition for a scalar product  $\langle | \rangle$ . Here, we define a scalar product  $\langle | \rangle$ , and motivate the choice. We have no compelling argument for the uniqueness of this scalar product, but we will show that it satisfies all consistency requirements so far considered. Therefore, it is reasonable to take it as a first ansatz.

Let us begin by considering an  $n$ -valent vertex. This can be arbitrarily expanded in trivalent vertices. Let  $i_1 \dots i_{n-3}$  be the colors of the internal edges, and let us represent by  $|i_1 \dots i_{n-3}\rangle$  the  $n$ -valent vertex expanded in trivalent vertices colored  $i_1 \dots i_{n-3}$ . We would like to determine an orthogonal basis from the quantities  $|i_1 \dots i_{n-3}\rangle$ . We have two highly non-trivial requirements. First, that this works independently from the way the  $n$ -valent vertex is expanded in trivalent ones. Second, that the volume be hermitian in this basis. Rather remarkably, we believe, both requirements can be satisfied.

Let us begin by considering a 4-valent vertex, for simplicity. There are two ways in which we can expand it in trivalent vertices. Thus, we have two distinct bases  $|i\rangle$  and  $|i'\rangle$  for the 4-valent vertices. If we wanted both of them to be orthonormal, the transformation between the two had to be given by a unitary matrix. Now, the transformation matrix between the two bases is provided by the recoupling theorem. The matrix is given by a Six-J symbol, seen as a matrix in its two rightmost entries. It is easy to see that this matrix is not unitary. However, we now show that we can rescale the length of the basis vectors  $|i\rangle$  in such a way that the transformation matrix becomes unitary (indeed, orthogonal). Indeed, let

$$n_j = \sqrt{\frac{\text{diagram with loop } j \text{ and edges } a, b, c, d}{\text{diagram with edges } a, b, c, d}}} \quad (8.1)$$

$$\tilde{n}_i = \sqrt{\frac{\text{diagram with loop } i \text{ and edges } a, b, c, d}{\text{diagram with edges } a, b, c, d}}} \quad (8.2)$$

In this basis, the recoupling theorem becomes

$$n_j = \sum_i \sqrt{\frac{\text{diagram with loops } j \text{ and } i \text{ and edges } a, b, c, d}{\text{diagram with edges } a, b, c, d}}} \begin{Bmatrix} a & b & i \\ c & d & j \end{Bmatrix} \tilde{n}_i$$



$$\begin{aligned}
&= \sum_i \sqrt{\frac{\text{Diagram 1}}{\text{Diagram 2}}} \cdot \tilde{\mathbf{n}}_i \\
&= \sum_i U(a, b, c, d)_j^i \tilde{\mathbf{n}}_i
\end{aligned} \tag{8.3}$$

Diagram 1: A trivalent vertex with external edges labeled  $a, b, c$  and internal edges labeled  $d, e, f$ . The vertex is represented by a square with a diagonal line from the top-left to the bottom-right. The top-left edge is labeled  $a$ , the top-right edge is labeled  $b$ , and the bottom-right edge is labeled  $c$ . The internal edges are labeled  $d, e, f$ .

Diagram 2: A trivalent vertex with external edges labeled  $a, b, c$  and internal edges labeled  $d, e, f$ . The vertex is represented by a square with a diagonal line from the top-left to the bottom-right. The top-left edge is labeled  $a$ , the top-right edge is labeled  $b$ , and the bottom-right edge is labeled  $c$ . The internal edges are labeled  $d, e, f$ .

We now prove that the matrix  $U(a, b, c, d)_j^i$  is real orthogonal. The inverse transformation matrix from the  $\tilde{\mathbf{n}}_i$  basis to the  $\mathbf{n}_j$  basis is given by the same expression (8.3), with a reordering of the external edges' colorings, i.e:

$$\tilde{\mathbf{n}}_k = \sum_i U(d, a, b, c)_i^k \mathbf{n}_k. \tag{8.4}$$

Therefore we have the relation

$$\sum_i U(a, b, c, d)_j^i U(d, a, b, c)_i^k = \delta_j^k \tag{8.5}$$

From direct inspection of eq. (8.3) it is easy to see that  $U(a, b, c, d)_k^i = U(d, a, b, c)_i^k$ . As an immediate consequence of eq. (8.5) we have orthogonality. Looking at eq. (E2) and (E4) we can easily compute the sign of the argument of the square root, which is:

$$\begin{aligned}
\text{sign}(\sqrt{\phantom{x}}) &= \frac{(-1)^i (-1)^j}{(-1)^{(a+b+j)/2 + (c+d+j)/2 + (a+d+i)/2 + (b+c+i)/2}} \\
&= (-1)^{a+b+c+d} = +1
\end{aligned} \tag{8.6}$$

We have thus shown that there exists a basis in which the recoupling theorem yields a unitary transformation. For higher valence vertices, the transformation from one trivalent expansion to another can be obtained by a repeated applications of the recoupling theorem transformation, and therefore by a product of orthogonal matrices. Thus, the argument above extends immediately to higher valence.

Now, the normalization we have found is exactly the one in which the volume operator is represented by a real antisymmetric matrix, as shown by eqs. (7.23) and (7.27). Therefore we have found a basis that satisfies all our requirements.

We thus define the normalized spin-network states by the following normalization: given an arbitrary spin-network state  $\langle S|$ , we label with an index  $i \in V$  all the 3-valent vertices of the expanded state (virtual and real)) and with a index  $e \in \mathcal{E}$  all its edges (virtual and real). We denote the color of the edge  $e$  by with  $p_e$  and the color of the three edges adjacent to the vertex  $i$  by  $a_i, b_i$  and  $c_i$ . We define the *normalized* spin network-state  $\langle S|_N$  by

$$\langle S|_N = \sqrt{\prod_{i \in V} \prod_{e \in \mathcal{E}} \frac{\Delta_{p_e}}{\theta(a_i, b_i, c_i)}} \langle S| \tag{8.7}$$

And we define a scalar product on  $\mathcal{V}$  by requiring that these states are orthonormal. We have immediately from the discussion above that the definition does not depend on the trivalent expansion chosen, and that the volume and area operators are symmetric with respect to this scalar product.

We think that the scalar product defined in this way is precisely the one defined on the loop representation by the loop transform [3,4] of the Ashtekar-Lewandowski measure [40], namely the conventional Haar measure lattice gauge theory scalar product for each graph. The precise relation is discussed by Reisenberger [25]. In turn, we expect that (the norm derived from) the scalar product we have defined is equivalent to the evaluation of the Kauffman bracket of the state, and to the trace of the Temperley-Lieb algebra, discussed in Appendix B.

## IX. CONCLUSIONS AND FUTURE DIRECTIONS

We have reviewed the loop representation of quantum gravity, and presented a number of novel results. We have made two modifications in the definition of the theory. First, we have inserted a minus sign in the definition of the loop observables. With this convention, the spinor identity is transformed into the binor identity, allowing immediately a local graphical calculus for the grasping operation and the use of recoupling theory. Second, we have defined the

loop operators by means of the parallel propagator of  $i$  times the Ashtekar connection, instead than just the Ashtekar connection. This second modification is substantial, because it yields quantum states that are eigenstates of area and volume with positive eigenvalues. We have shown that the loop states obey the axioms of recoupling theory, and the corresponding graphical formalism provides a powerful tool for computing the action of geometrical operators. We have discussed in detail the way in which recoupling theory can be used in this context.

Using recoupling theory, we have re-derived known results on the eigenstates of the area, and the volume of trivalent and 4-valent vertices. We have given a general expression for the volume of higher valence vertices. We have proven that the square root in the volume operator is well defined, because the relevant operator is hermitian. We have defined a scalar product by a suitable normalization of the trivalent spin networks. We have shown that that the scalar product is well defined and independent from the trivalent expansion chosen, and that the volume is symmetric with respect to this scalar product.

Notice that the area and volume operators  $\hat{A}$  and  $\hat{V}$  do *not* correspond to physical observables: they are not gauge invariant and do not commute with GR's constraints. The areas and volumes that we routinely measure are associated to spatial regions determined by matter. Indeed, the area and volume of regions determined by physical matter *are* represented on the phase space of the coupled gravity-matter theory by observables which are gauge invariant (see for instance [41]). However, it was suggested in Ref. [16] that it is reasonable to expect that these physical areas and volumes (of spatial regions determined by matter) be *still* expressed by (operators unitary equivalent to)  $\hat{A}$  and  $\hat{V}$ . See Refs. [41] and [16] for the details of the argument. If this suggestion is correct, the spectra computed here can be taken as physical predictions on short scale geometry, following from the loop representation of quantum gravity [16]. These predictions are testable in principle, and could perhaps lead to observable consequences.

We consider the following open problems particularly important for the development of the theory.

- We have not explored the degenerate cases in the action of the area operator (see section VI).
- We believe that the formalism is now well established for a precise discussion of the Hamiltonian and for computing transition amplitudes [19,20].
- Can a weave [13] be found for which not just the area but the volume as well approximates smooth geometries? Can a weave related to a four dimensional geometry [42] be constructed?
- A way of implementing the Lorentzian reality conditions is, to our knowledge, still lacking (For an attempt to address this problem, see [43]).
- Under the optimistic assumption that the above technical problems could be addressed, a possible first task for the theory could be the following. Compute the clock time evolution of a weave representing a black hole; show that Hawking's radiation [44] is emitted, and determine the final stage of the black hole after evaporation.
- Supposing that area and volume eigenvalues computed here describe an actual physical discreteness (in the quantum sense) of Planck scale geometry, could there be any low energy observable consequence of such discreteness?

## ACKNOWLEDGMENTS

We thank Mike Reisenberger and Lee Smolin for teaching us the relevance of recoupling theory and of its tangle theoretical version; Roumen Borissov, Viqar Husain and Renate Loll for a careful reading of the manuscript and many suggestions; Seth Major and Simonetta Frittelli for comments and suggestions, and Abhay Ashtekar for valuable criticisms and insights. One of us (RDP) thanks the members of the Relativity group of Pittsburgh –where this work begun– for their warm hospitality, as well as Massimo Pauri and Luca Lusanna for their continuous support and encouragement during these years. This work has been partially supported by the NSF grant PHY-90-12099 (USA), by the INFN grant “Iniziativa specifica FI-2” (Italy), and by the Human Capital and Mobility Program “Constrained Dynamical Systems” (European Union).

## APPENDIX A: PAULI MATRICES IDENTITIES

Defining  $\tau_i = -\frac{i}{2} \sigma_i$ , where  $\sigma_i$  are the Pauli matrices, we have the following identities:

$$\text{Tr}[\tau_i \tau_j] = -\frac{1}{2} \delta_{ij}, \quad (\text{A1})$$

$$\text{Tr}[\tau_i \tau_j \tau_k] = -\frac{1}{4} \epsilon_{ijk}, \quad (\text{A2})$$

$$\delta^{ij} \tau_i^A{}^B \tau_j^C{}^D = -\frac{1}{4} (\delta_A^D \delta_B^C - \epsilon^{BD} \epsilon_{AC}), \quad (\text{A3})$$

$$\delta^{ij} \text{Tr}[A \tau_i] \text{Tr}[B \tau_j] = -\frac{1}{4} \{ \text{Tr}[AB] - \text{Tr}[AB^{-1}] \}, \quad (\text{A4})$$

$$A^{-1}{}^A{}^B = \epsilon^{BD} \epsilon_{AC} A_D^C, \quad (\text{A5})$$

$$\delta_A^B \delta_D^C = \delta_A^C \delta_D^B + \epsilon^{BC} \epsilon_{AD}, \quad (\text{A6})$$

$$\text{Tr}[A] \text{Tr}[B] = \text{Tr}[AB] + \text{Tr}[AB^{-1}], \quad (\text{A7})$$

where  $A$  and  $B$  are  $SL(2, C)$  matrices.

## APPENDIX B: KAUFFMAN BRACKETS AND TEMPERLEY-LIEB RECOUPLING THEORY

In the context of Knot theory [24], the appearance of recoupling theory is based on the observation that the Kauffman bracket satisfies the properties (and is completely determined by the properties)

$$\langle \begin{array}{c} \diagup \quad \diagdown \\ \diagdown \quad \diagup \end{array} \rangle = A \langle \begin{array}{c} \cup \\ \cap \end{array} \rangle + A^{-1} \langle \begin{array}{c} | \\ | \end{array} \rangle \quad (\text{B1})$$

and

$$\langle \bigcirc \cup \mathbf{K} \rangle = d \langle \mathbf{K} \rangle \quad (\text{B2})$$

where  $\langle \rangle$  denotes the Kauffman bracket, where  $d = -A^2 - A^{-2}$  and  $\mathbf{K}$  is any diagram that does not intersect the added loop. These properties of the Kauffman bracket are sufficient to generate the entire formalism of recoupling theory. In particular, they generate a “tangle theoretic” interpretation of the Temperley-Lieb algebra as follows.

A planar tangle is a set of lines on a plane. It is possible to write an arbitrary tangle inside the Kauffman brackets as the sum of non-intersecting tangles by applying eq. (B1) to all crossings. In [45] it is shown that every planar non intersecting  $n$ -tangle with  $n$  inputs and  $n$  outputs is equivalent to the product of elementary tangles  $\mathbb{1}_n, U_1, \dots, U_{n-1}$ , given by

$$\begin{aligned} \boxed{\mathbb{1}_n} &= \text{|||||} \\ \boxed{U_1} &= \begin{array}{c} \cup \\ \cap \end{array} \text{||||} \\ &\vdots \\ \boxed{U_{n-1}} &= \text{||||} \begin{array}{c} \cup \\ \cap \end{array} \end{aligned}$$

where the product is interpreted as a stacking of two diagrams. Two such products represent tangles equivalent under the Kauffman brackets if and only they can be transformed into each other by the relations

$$U_i^2 = d U_i \quad (\text{B3})$$

$$U_i U_{i\pm 1} U_i = U_i \quad (\text{B4})$$

$$U_i U_j = U_j U_i \quad , \quad |i - j| > 1 \quad , \quad (\text{B5})$$

which are at the basis of the Temperley-Lieb algebra. For example (B3), means:

$$\begin{array}{c} \boxed{U_1} \\ \boxed{U_1} \end{array} = \begin{array}{c} \cup \\ \cap \end{array} \text{|||} = \begin{array}{c} \cup \\ \cap \end{array} \text{|||} = d \boxed{U_1}. \quad (\text{B6})$$

Given an  $n$ -tangle  $\mathbf{x}$ , let  $\bar{\mathbf{x}}$  denote the standard closure of  $\mathbf{x}$ , obtained by attaching the  $k^{th}$  input to the  $k^{th}$  output.

The Temperley-Lieb algebra  $T_n$  is the free additive algebra over  $\tilde{Z}[A, A^{-1}]$  with multiplicative generators  $\mathbb{1}_n, U_1, \dots, U_{n-1}$ . The trace on the algebra  $T_n$  is defined by:

- (i) If  $\mathbf{x}$  is an  $n$ -tangle then  $tr(\mathbf{x}) = \langle \bar{\mathbf{x}} \rangle$  where  $\langle \rangle$  denotes the Kauffman bracket, or, which is the same, the recursive evaluation of  $\bar{\mathbf{x}}$  using (B1) and (B2) .
- (ii)  $tr(\mathbf{x} + \mathbf{y}) = tr(\mathbf{x}) + tr(\mathbf{y})$ .

### 1. The Jones-Wenzel projector

It can be shown [24] that in the Temperley-Lieb algebra  $T_n$  there exist one (and only one) element  $\Pi_n \in T_n$  such that  $\Pi_n^2 = \Pi_n$  and  $\Pi_n U_i = U_i \Pi_n, i = 1, \dots, n-1$ . This unique element it is called the Jones-Wenzel projector of  $T_n$ . Its explicit expression is given by:

$$\Pi_n = \frac{\boxed{n}}{\boxed{1}} = \frac{1}{n!} \sum_p (A^{-3})^{|p|} P_n^{(p)}. \quad (\text{B7})$$

$P(p), p = 1 \dots n!$  is the  $n$ -tangle obtained by all possible permutations  $p$  in the way the  $n$  lines entering  $e$  are connected to the  $n$  outgoing lines,  $P_n^{(p)}$  its a minimal representation of the permutation  $(p)$ , and  $|p|$  its the parity of the representation. Since any  $n$ -tangle can be expanded, using eq. (B1), in a sum of *non-intersecting* tangles, the expression (B7) is an elements of  $T_n$ . As an example we give the definition of  $\Pi_2$ :

$$\begin{aligned} \Pi_2 &= \frac{\boxed{2}}{\boxed{1}} = \frac{1}{\{2\}!} \left[ \begin{array}{c} | \\ | \end{array} + A^{-3} \begin{array}{c} \diagup \diagdown \end{array} \right] \\ &= \frac{1}{1 + A^{-4}} \left[ \begin{array}{c} | \\ | \end{array} + A^{-4} \begin{array}{c} | \\ | \end{array} + A^{-2} \begin{array}{c} \cup \\ \cup \end{array} \right] \\ &= \begin{array}{c} | \\ | \end{array} + \frac{1}{A^2 + A^{-2}} \begin{array}{c} \cup \\ \cup \end{array} \\ &= \begin{array}{c} | \\ | \end{array} - \frac{1}{d} \begin{array}{c} \cup \\ \cup \end{array} = \mathbb{1}_2 - \frac{1}{d} U_1. \end{aligned}$$

In the  $A = -1$  case the projectors reduce to antisymmetrizers.

### 2. A special sum of tangles: the three vertex

A special sum of tangles is indicated by a 3-vertex. Each line of the vertex is labeled with a positive integer  $a, b$  or  $c$  as shown below



and it is assumed that  $m = (a+b-c)/2, n = (b+c-a)/2$  and  $p = (c+a-b)/2$  are positive integer. This last condition is called the *admissibility condition* for the 3-vertex  $(a, b, c)$ . A line labeled by a positive integer  $a$  is interpreted as the non-intersecting  $n$ -tangle  $\mathbb{1}_a$ . The 3-vertex is then defined as:

$$\begin{array}{c} a \quad b \\ \diagdown \quad \diagup \\ \bullet \\ | \\ c \end{array} \stackrel{def}{=} \begin{array}{c} a \quad b \\ \diagdown \quad \diagup \\ \boxed{m} \quad \boxed{n} \\ \diagup \quad \diagdown \\ \boxed{p} \\ | \\ c \end{array} \quad (\text{B8})$$

Here, it is understood that each Temperley-Lieb projector is fully expanded. For instance

$$\begin{aligned}
\begin{array}{c} 1 \quad 1 \\ \diagdown \quad \diagup \\ \bullet \\ \diagup \quad \diagdown \\ 2 \end{array} &= \begin{array}{c} \diagdown \quad \diagup \\ \parallel \quad \parallel \\ \diagup \quad \diagdown \end{array} - \frac{1}{d} \begin{array}{c} \diagdown \quad \diagup \\ \cap \\ \diagup \quad \diagdown \end{array} + \\
\begin{array}{c} 2 \quad 2 \\ \diagdown \quad \diagup \\ \bullet \\ \diagup \quad \diagdown \\ 2 \end{array} &= \begin{array}{c} \diagdown \quad \diagup \\ \parallel \quad \parallel \\ \diagup \quad \diagdown \end{array} + \frac{2}{d^2} \begin{array}{c} \diagdown \quad \diagup \\ \cap \\ \diagup \quad \diagdown \end{array} \\
&\quad - \frac{1}{d} \left[ \begin{array}{c} \diagdown \quad \diagup \\ \parallel \quad \parallel \\ \diagup \quad \diagdown \end{array} + \begin{array}{c} \diagdown \quad \diagup \\ \cap \\ \diagup \quad \diagdown \end{array} + \begin{array}{c} \diagdown \quad \diagup \\ \parallel \quad \parallel \\ \diagup \quad \diagdown \end{array} \right]
\end{aligned}$$

### 3. Chromatic evaluation

If we joining trivalent vertices by their edges, we obtain trivalent networks. Thus, in the present context a trivalent spin network is defined as a trivalent graph with an admissible coloring. Notice that in this context spin networks are not embedded in a three dimensional space. An edge of color  $n$  represents  $n$  parallel lines and a Jones-Wenzel projector, and a vertex is understood as completed expanded in terms of non-intersecting tangles, as above. Thus, a trivalent spin network determines a closed tangle. We can compute the Kauffman bracket, or the Temperley-Lieb trace, of such tangle. This is also called the chromatic evaluation, or network evaluation. The explicit calculation of the trace is generally based on a generalization of the chromatic method of spin-network evaluation [46]. In ref. [46] this method is used in order to compute the Clebsch-Gordon coefficients for the group  $SU(2)$ .

Chromatic evaluations of simple networks are given in Appendix E. We refer to [24] for the details of the computations. Here, we perform one such computation explicitly, as an example. Let us consider the spin network formed by two trivalent vertices joined to each other. This is called the  $\theta$  network. Consider the case with edges of color 2, 1, 1:

$$\begin{aligned}
\begin{array}{c} 1 \\ \hline \begin{array}{c} 2 \\ \hline 1 \end{array} \end{array} &= \begin{array}{c} 1 \\ \hline \begin{array}{c} \text{JW projector} \\ \hline 1 \end{array} \end{array} = \begin{array}{c} 1 \\ \hline \begin{array}{c} 2 \\ \hline 1 \end{array} \end{array} - \frac{1}{d} \begin{array}{c} 1 \\ \hline \begin{array}{c} \text{JW projector} \\ \hline 1 \end{array} \end{array} = \\
&= d^2 - \frac{1}{d}d = d^2 - 1 = (- (A^2 + A^{-2}))^2 - 1 = \\
&= [3] = \frac{(-1)^{0+1+1} [3]! [1]! [1]! [0]!}{[2]! [1]! [1]!}.
\end{aligned} \tag{B9}$$

We have: (1) expanded the trivalent vertices explicitly; (2) computed the trace using (B2); (3) written the expression in terms of quantum integer (E1); (4) compared the result with the general formula of the chromatic evaluation of the  $\theta$  net (E4). In the  $A = -1$  case, the above gives

$$\begin{array}{c} 1 \\ \hline \begin{array}{c} 2 \\ \hline 1 \end{array} \end{array} = 3. \tag{B10}$$

## APPENDIX C: PENROSE THEORY OF SPIN-NETWORK

In this appendix we discuss the relation between the Penrose theory of spin networks and the Kauffman bracket and Temperley-Lieb recoupling theory. This appendix is based essentially on Penrose's original formulation [30] and on an article by Kauffman [47]. A basic idea used by Penrose (in his doctoral thesis) it is to rewrite any tensor expression in which there are sums of indices in a graphical way [23]. Consider the calculus of spinors. Penrose represents the basic element of spinor calculus as

$$\delta_C^A = \begin{array}{c} \bullet^A \\ | \\ \bullet_C \end{array} \quad (C1a)$$

$$\epsilon_{AC} = \begin{array}{c} \bullet^A \\ \curvearrowright \\ \bullet_C \end{array} \quad \epsilon^{AC} = \begin{array}{c} \bullet^A \\ \curvearrowleft \\ \bullet_C \end{array} \quad (C1b)$$

$$\eta_A = \begin{array}{c} \boxed{\eta} \\ \bullet_A \end{array} \quad \eta^A = \begin{array}{c} \bullet^A \\ \boxed{\eta} \end{array} \quad (C1c)$$

and generally to any tensor object

$$X_{AB}^C = \begin{array}{c} \bullet^C \\ \boxed{X} \\ \bullet_A \bullet_B \end{array} \quad (C1d)$$

This convention provides the possibility of writing the product of any two tensors in a graphical way. For example:

$$\epsilon_{AB} \eta^A \eta^B = \begin{array}{c} \bullet^A \quad \bullet^B \\ \boxed{\eta} \quad \boxed{\eta} \end{array} \quad (C2)$$

$$= -\epsilon_{AD} \epsilon_{BC} \epsilon^{CD} \eta^A \eta^B = - \begin{array}{c} \bullet^A \quad \bullet^B \quad \bullet^C \quad \bullet^D \\ \boxed{\eta} \quad \boxed{\eta} \quad \curvearrowright \end{array} \quad (C3)$$

$$= -\epsilon_{CD} \delta_A^D \delta_B^C \eta^A \eta^B = - \begin{array}{c} \bullet^C \quad \bullet^D \\ \diagdown \quad \diagup \\ \boxed{\eta} \quad \boxed{\eta} \end{array} \quad (C4)$$

In the light of the example above, Penrose considered a modification of the spinor calculus, which he denoted as binor calculus. The binor calculus is obtained by adding two conventions to the calculus above:

1. Assign a minus sign to each minimum.
2. Assign a minus sign to each crossing
3. Maxima and minima are taken with respect to a fixed direction in the plane. (This direction is conventionally taken to be the vertical direction on the written page)
4. A segment with transversal intersection with all horizontal direction is taken to be a Kronecker delta.

The advantage of these additional rules is that they make the calculus topological invariant, namely one can arbitrarily smoothly deform a graphical expression without changing its meaning.

The other way around, any curve can now be decomposed in a product of  $\delta$ 's and  $\epsilon$ 's and any two curves that are ambient isotopic, i.e. that can be transformed one in the other by a sequence of Reidemeister moves, represent the tensorial expression as product of epsilons and deltas.

A closed loop (with this convention) has value  $(-2)$ , because

$$\bigcirc = -\epsilon_{AB} \epsilon^{AB} = -2 \quad (C5)$$

and we have the basic binor identity, which reads:

$$\begin{array}{c} \times \\ + \\ | \quad | \\ + \\ \smile \end{array} = (-1) \delta_B^C \delta_A^D + \delta_A^C \delta_B^D + (-1) \epsilon_{AB} \epsilon^{CD} = 0 \quad (C6)$$

It is easy to see that these relations are exactly the same as the properties (B1) and (B2) of the Kauffman bracket with  $A = -1$  and  $d = -2$ . Notice from equation (B1) that if  $A = -1$  undercrossing and overcrossing are equivalent: indeed they give the same expansion. Clearly in Penrose's binor calculus there is no meaning of the distinction between over and under crossing. The theory can then be developed as the recoupling theory of appendix B with the special value  $A = -1$ . Thus, the  $A = -1$  Kauffman bracket of a spin network is the same as the Penrose's spin network evaluation.

For more detail on the exact relation between *tangle-theoretic* recoupling theory and spin-networks see, for example, [47,33,24]. An important point that emerges from this brief discussion is the possibility of using a topological invariant calculus for writing generic  $SL(2, C)$  invariant tensor expressions. (This was one of the original motivations of Penrose for introducing binors.) It is possible to write any  $SL(2, C)$  Mandelstam identities (3.3) in a graphical way and in particular we can express these identities in spin-network-like graphical relations, in which each edge is the antisymmetrization of the holonomies along the edge.

## APPENDIX D: GRAPHICAL CALCULUS OF ANGULAR MOMENTUM AND ITS RELATION WITH THE TANGLE-THEORETICAL RECOUPLING THEORY

Finally, the  $A = -1$  case of recoupling theory is equivalent to the graphical calculus of the algebra of the  $SU(2)$  representations. In the literature there is a great number of results on the Wigner  $3nJ$  symbols and a well developed theory of graphical calculus for angular momentum. To our knowledge the most used graphical method of computation in the representation theory of  $su(2)$  are the one due to Levinson [48] and developed by Yutsis, Levinson and Vanagas [49] and the slightly modified version of Brink and Satcheler [39]. We discuss here the connection between the tangle-theoretical recoupling theory (in the case  $A = 1$ )<sup>8</sup> and the graphical method of Brink and Satcheler [39]. We indicate a diagram in the Brink convention with a subscript  $B$ , and the  $3nJ$ -Symbol (in the standard normalization<sup>9</sup>) with a subscript  $W$ . The two methods are identical up to a different normalization of the 3-valent vertex and the fact the the orientations of any vertex are explicit denoted with a  $+$  for a counter-clockwise orientation and  $-$  for a clockwise one. (In this appendix we are imprecise about this overall sign.) Following Kauffman, we have chosen to denote the recoupling matrix of a 4-valent node by curl brackets, while curl brackets are used in the angular momentum literature to indicate Wigner's  $6J$ -symbols, which are the evaluation of the tetragonal net. In other words, the Wigner  $3J$  and  $6J$ -symbol are defined as the evaluation

$$\{a, b, c\}_W = \text{norm} \cdot \theta(a, b, c), \quad (\text{D1})$$

$$\left\{ \begin{array}{ccc} a & b & c \\ d & e & f \end{array} \right\}_W = \text{norm} \cdot Tet \left[ \begin{array}{ccc} a & b & c \\ d & e & f \end{array} \right], \quad (\text{D2})$$

where the normalization factor “norm” of [39] corresponds to the choice

$$\{a, b, c\}_W = \left( \begin{array}{c} \text{---} a \text{---} \\ \text{---} b \text{---} \\ \text{---} c \text{---} \end{array} \right)_B = +1 \quad (\text{D3})$$

This is also the standard normalization of the Clebsh-Gordon coefficient that gives the usual normalization of the Wigner  $3nJ$ -Symbol. With this normalization the recoupling theorem (eq. (E5)) becomes:

$$\begin{aligned} \left( \begin{array}{ccc} b & & c \\ & j & \\ a & & d \end{array} \right)_B &= \\ &= \sum_i \Delta_i \left\{ \begin{array}{ccc} a & b & i \\ c & d & j \end{array} \right\}_W \left( \begin{array}{ccc} b & & c \\ & i & \\ a & & d \end{array} \right)_B, \end{aligned} \quad (\text{D4})$$

where  $\Delta_i$  is interpreted as the dimension of the representation of spin  $i/2$ . From eqs. (D3) and (D4) we have the correspondence between a Brink diagram and one of ours: one has to divide any 3-valent node by  $\sqrt{\theta(a, b, c)}$ . As an example, let us consider the relation between the tetrahedron evaluation ( $Tet$ ) and the Wigner  $6J$  symbol.

$$\left\{ \begin{array}{ccc} A & B & E \\ C & D & F \end{array} \right\}_W = \left( \begin{array}{ccc} B & & C \\ & F & \\ A & & D \end{array} \right)_B \quad (\text{D5})$$

---

<sup>8</sup>The correspondence between the case  $A = -1$  and  $A = 1$  and their equivalence is discussed by R. Penrose in [23].

<sup>9</sup>We recall the fact that we use color and not spin to denote the  $su(2)$  representation associated to an edge. In the angular momentum literature, the spin notation is prevalent. As a consequence, numbers in Brink diagrams, or in  $3nJ$ -Symbols in standard normalization, must be understood as the spin of the edge; or, equivalently, the color divided by two.

$$\begin{aligned}
&= \frac{\text{Diagram: A diamond shape with vertices A (bottom), B (top), C (right), D (left). Internal lines connect A-B, B-C, C-D, D-A. A horizontal line F connects B and C. A vertical line E connects C and D.}}{\sqrt{\text{Diagram: Four circles in a row. Circle 1: A (top), B (middle), F (bottom). Circle 2: C (top), D (middle), F (bottom). Circle 3: A (top), D (middle), E (bottom). Circle 4: B (top), C (middle), E (bottom).}}} \\
&= \frac{\text{Diagram: Tetrahedron with vertices A, B, C, D, E, F.}}{\sqrt{\theta(A, B, F)\theta(C, D, F)\theta(A, D, E)\theta(B, C, E)}}.
\end{aligned}$$

## APPENDIX E: BASIC FORMULAS OF RECOUPLING THEORY

We collect here the basic formulas of recoupling theory in the case  $A = -1$  and  $d = -2$ . Using the “quantum” integer

$$\begin{aligned}
[n] &= \frac{A^{2n} - A^{-2n}}{A^2 - A^{-2}} = (-1)^{n-1} \Delta_{n-1} = n \\
\{n\} &= \frac{1 - A^{-4n}}{1 - A^{-4}} = A^{2n-2} [n] = n \\
\{n\}! &= \{1\} \cdot \{2\} \cdots \{n\} = n!
\end{aligned} \tag{E1}$$

we define

(1) The symmetrizer

$$\Delta_n = \text{Diagram: A circle with a vertical line segment at the bottom, labeled n.} = (-1)^n [n+1] = (-1)^n (n+1). \tag{E2}$$

(2) The exchange of line in a 3-Vertex

$$\text{Diagram: A 3-vertex with lines a, b, c. Line c is at the bottom, a and b are at the top.} = \lambda_c^{ab} \text{Diagram: A 3-vertex with lines a, b, c. Line c is at the bottom, a and b are at the top, but a and b are swapped.} \tag{E3}$$

Where  $\lambda_c^{ab} = (-1)^{(a+b-c)/2} A^{(a'+b'-c')/2}$ , and  $x' = x(x+2)$ .

(3) The  $\theta$  evaluation

$$\begin{aligned}
\theta(a, b, c) &= \text{Diagram: A circle with three horizontal lines inside, labeled a (top), b (middle), c (bottom).} \\
&= \frac{(-1)^{m+n+p} [m+n+p+1]! [m]! [p]! [p]!}{[a]! [b]! [c]!}
\end{aligned} \tag{E4}$$

where  $m = (a+b-c)/2$ ,  $n = (b+c-a)/2$ ,  $p = (c+a-b)/2$ .

(4) The recoupling theorem:

$$\text{Diagram: A 3-vertex with lines a, b, c. Line a is at the bottom, b and c are at the top.} = \sum_i \left\{ \begin{matrix} a & b & i \\ c & d & j \end{matrix} \right\} \text{Diagram: A 3-vertex with lines a, b, c. Line a is at the bottom, b and c are at the top, but b and c are swapped.} \tag{E5}$$

$$\left\{ \begin{matrix} a & b & i \\ c & d & j \end{matrix} \right\} = \frac{\Delta_i \text{Diagram: Tetrahedron with vertices a, b, c, d, i, j.}}{\theta(a, d, i)\theta(b, c, i)}. \tag{E6}$$



(5) The Tetrahedral net

$$\begin{aligned}
 Tet \begin{bmatrix} A & B & E \\ C & D & F \end{bmatrix} &= \begin{array}{c} \begin{array}{ccc} & B & C \\ & \nearrow & \searrow \\ A & F & D \\ & \nwarrow & \nearrow \\ & D & E \end{array} \\ \end{array} \\
 &= \frac{\mathcal{I}}{\mathcal{E}} \sum_{m \leq S \leq M} \frac{(-1)^S [S]!}{\prod_i [S - a_i]! \prod_j [b_j - S]!} ,
 \end{aligned} \tag{E7}$$

where

$$\begin{aligned}
 a_1 &= \frac{A + D - E}{2}, & b_1 &= \frac{B + D + E + F}{2}, \\
 a_2 &= \frac{B + C - E}{2}, & b_2 &= \frac{A + C + E + F}{2}, \\
 a_3 &= \frac{A + B - F}{2}, & b_3 &= \frac{A + B + C + D}{2}, \\
 a_4 &= \frac{C + D - F}{2},
 \end{aligned}$$

$$\begin{aligned}
 m &= \max\{a_i\}, & M &= \min\{b_j\}, \\
 \mathcal{E} &= [A]! [B]! [C]! [D]! [E]! [F]!, & \mathcal{I} &= \prod_{ij} [b_j - a_i]! .
 \end{aligned}$$

(6) The reduction formula

$$\begin{array}{c} \begin{array}{c} |a \\ \circlearrowleft \\ b \\ \circlearrowright \\ |a \end{array} \end{array} = \frac{\begin{array}{c} \begin{array}{c} a \\ \circlearrowleft \\ b \\ \circlearrowright \\ c \\ \circlearrowleft \\ a \end{array} \end{array}}{\begin{array}{c} \begin{array}{c} a \\ \circlearrowleft \\ a \end{array} \end{array}} \cdot \left| a \right. \tag{E8}$$

$$\begin{array}{c} \begin{array}{c} \begin{array}{ccc} & a & \\ b & \nearrow & d \\ & f & \\ c & \nwarrow & e \\ & a & \end{array} \end{array} = \frac{\begin{array}{c} \begin{array}{ccc} c & d & \\ \nearrow & f & \searrow \\ b & e & \\ \nwarrow & & \nearrow \end{array} \end{array}}{\begin{array}{c} \begin{array}{c} a \\ \circlearrowleft \\ a \end{array} \end{array}} \cdot \left| a \right. . \tag{E9}$$

These formulas are sufficient for the computations performed in the paper. For details on their derivation, see [24].

## APPENDIX F: SOME VOLUME EIGENVALUES

Finally, we present here some volume eigenvalues of four- and five-valent vertices. The tables give the colors of the external edges, the dimension of the vertex (number of independent compatible colorings), and the eigenvalues. The number in parenthesis indicates the multiplicity of the eigenvalues.

$P_0$	$P_1$	$P_2$	$P_3$	Dim.	$\lambda_{\beta_i} = \lambda_{\beta_i}(P_0, \dots, P_3)$
1	1	1	1	2	(2) $\sqrt{\frac{1}{8}\sqrt{3}}$
2	2	2	2	3	(1) 0, (2) $\sqrt{\frac{1}{2}\sqrt{3}}$
3	3	3	3	4	(2) $\sqrt{\frac{3}{8}\sqrt{3}}$ , (2) $\sqrt{\frac{3}{8}\sqrt{35}}$
4	4	4	4	5	(1) 0 (2) $\sqrt{\frac{3}{4}\sqrt{22 - \sqrt{114}}}$ , (2) $\sqrt{\frac{3}{4}\sqrt{22 + \sqrt{114}}}$

5	5	5	5	6	(2) $\sqrt{\frac{1}{8}\sqrt{1155}},$
					(2) $\sqrt{\frac{1}{8}\sqrt{2211-96\sqrt{481}}}$
					(2) $\sqrt{\frac{1}{8}\sqrt{2211+96\sqrt{481}}}$
6	6	6	6	7	(1) 0,
					(2) $\sqrt{2\sqrt{3}},$
					(2) $\sqrt{\frac{9}{2}\sqrt{3}},$
					(2) $\sqrt{\frac{1}{2}\sqrt{723}}$
<hr/>					
1	1	1	1	2	(2) $\sqrt{\frac{1}{8}\sqrt{3}}$
2	2	1	1	2	(2) $\sqrt{\frac{1}{4}\sqrt{2}}$
3	2	2	1	2	(2) $\sqrt{\frac{1}{4}\sqrt{5}}$
3	3	1	1	2	(2) $\sqrt{\frac{1}{8}\sqrt{15}}$
3	3	3	1	2	(2) $\sqrt{\frac{1}{2}\sqrt{3}}$
4	2	2	2	2	(2) $\sqrt{\frac{1}{2}\sqrt{2}}$
4	3	2	1	2	(2) $\sqrt{\frac{3}{4}}$
4	4	1	1	2	(2) $\sqrt{\frac{1}{4}\sqrt{6}}$
4	4	3	1	2	(2) $\sqrt{\frac{1}{4}\sqrt{21}}$
5	3	2	2	2	(2) $\sqrt{\frac{1}{4}\sqrt{21}}$
5	3	3	1	2	(2) $\sqrt{\frac{3}{8}\sqrt{7}}$
5	4	2	1	2	(2) $\sqrt{\frac{1}{4}\sqrt{14}}$
5	4	4	1	2	(2) $\sqrt{\frac{3}{2}}$
5	5	1	1	2	(2) $\sqrt{\frac{1}{8}\sqrt{35}}$
5	5	3	1	2	(2) $\sqrt{\sqrt{2}}$
5	5	5	1	2	(2) $\sqrt{\frac{9}{8}\sqrt{3}}$
6	4	2	2	2	(2) $\sqrt{2}$
6	4	3	1	2	(2) $\sqrt{\frac{1}{2}\sqrt{6}}$
6	5	2	1	2	(2) $\sqrt{\frac{1}{2}\sqrt{5}}$
6	5	4	1	2	(2) $\sqrt{\frac{3}{4}\sqrt{6}}$
6	6	1	1	2	(2) $\sqrt{\frac{1}{2}\sqrt{3}}$
6	6	3	1	2	(2) $\sqrt{\frac{3}{4}\sqrt{5}}$
6	6	5	1	2	(2) $\sqrt{\frac{3}{4}\sqrt{10}}$
7	3	3	3	2	(2) $\sqrt{\frac{9}{8}\sqrt{3}}$
7	4	3	2	2	(2) $\sqrt{\frac{3}{4}\sqrt{6}}$
7	4	4	1	2	(2) $\sqrt{\frac{3}{2}}$
7	5	2	2	2	(2) $\sqrt{\frac{3}{2}\sqrt{5}}$
7	5	3	1	2	(2) $\sqrt{\frac{3}{8}\sqrt{15}}$
7	5	5	1	2	(2) $\sqrt{\sqrt{5}}$
7	6	2	1	2	(2) $\sqrt{\frac{3}{4}\sqrt{3}}$
7	6	4	1	2	(2) $\sqrt{\frac{5}{4}\sqrt{3}}$

7	6	6	1	2	(2) $\sqrt{\frac{1}{2}\sqrt{33}}$
7	7	1	1	2	(2) $\sqrt{\frac{3}{8}\sqrt{7}}$
7	7	3	1	2	(2) $\sqrt{\frac{1}{2}\sqrt{15}}$
7	7	5	1	2	(2) $\sqrt{\frac{3}{8}\sqrt{55}}$
7	7	7	1	2	(2) $\sqrt{2\sqrt{3}}$
8	4	3	3	2	(2) $\sqrt{\frac{3}{4}\sqrt{10}}$
8	4	4	2	2	(2) $\sqrt{\sqrt{5}}$
<hr/>					
2	2	2	2	3	(1) 0, (2) $\sqrt{\frac{1}{2}\sqrt{3}}$
3	3	2	2	3	(1) 0, (2) $\sqrt{\frac{1}{4}\sqrt{26}}$
4	3	3	2	3	(1) 0, (2) $\sqrt{\frac{3}{4}\sqrt{6}}$
4	4	2	2	3	(1) 0, (2) $\sqrt{\frac{1}{2}\sqrt{11}}$
4	4	4	2	3	(1) 0, (2) $\sqrt{\frac{3}{2}\sqrt{3}}$
5	3	3	3	3	(1) 0, (2) $\sqrt{\frac{3}{2}\sqrt{3}}$
5	4	3	2	3	(1) 0, (2) $\sqrt{\frac{1}{4}\sqrt{89}}$
5	5	2	2	3	(1) 0, (2) $\sqrt{\frac{1}{4}\sqrt{66}}$
5	5	4	2	3	(1) 0, (2) $\sqrt{\frac{1}{4}\sqrt{174}}$
6	4	3	3	3	(1) 0, (2) $\sqrt{\frac{1}{4}\sqrt{174}}$
6	4	4	2	3	(1) 0, (2) $\sqrt{3}$
6	5	3	2	3	(1) 0, (2) $\sqrt{\frac{1}{4}\sqrt{131}}$
6	5	5	2	3	(1) 0, (2) $\sqrt{\frac{1}{2}\sqrt{69}}$
6	6	2	2	3	(1) 0, (2) $\sqrt{\frac{1}{2}\sqrt{23}}$
6	6	4	2	3	(1) 0, (2) $\sqrt{\frac{3}{2}\sqrt{7}}$
6	6	6	2	3	(1) 0, (2) $\sqrt{3\sqrt{3}}$
7	4	4	3	3	(1) 0, (2) $\sqrt{\frac{1}{2}\sqrt{69}}$
7	5	3	3	3	(1) 0, (2) $\sqrt{\frac{3}{2}\sqrt{7}}$
7	5	4	2	3	(1) 0, (2) $\sqrt{\frac{1}{4}\sqrt{209}}$
7	6	3	2	3	(1) 0, (2) $\sqrt{\frac{3}{2}\sqrt{5}}$
7	6	5	2	3	(1) 0, (2) $\sqrt{\frac{1}{4}\sqrt{395}}$
7	7	2	2	3	(1) 0, (2) $\sqrt{\frac{1}{4}\sqrt{122}}$
7	7	4	2	3	(1) 0, (2) $\sqrt{\frac{3}{4}\sqrt{38}}$
7	7	6	2	3	(1) 0, (2) $\sqrt{\frac{3}{2}\sqrt{17}}$
<hr/>					
3	3	3	3	4	(2) $\sqrt{\frac{3}{8}\sqrt{3}},$
					(2) $\sqrt{\frac{3}{8}\sqrt{35}}$
4	4	3	3	4	(2) $\sqrt{\frac{3}{4}\sqrt{9-\sqrt{57}}},$
					(2) $\sqrt{\frac{3}{4}\sqrt{9+\sqrt{57}}}$
5	4	4	3	4	(2) $\sqrt{\frac{3}{8}\sqrt{66-2\sqrt{753}}},$
					(2) $\sqrt{\frac{3}{8}\sqrt{66+2\sqrt{753}}}$

5	5	3	3	4	(2) $\sqrt{\frac{1}{8}\sqrt{511-16\sqrt{721}}}$ , (2) $\sqrt{\frac{1}{8}\sqrt{511+16\sqrt{721}}}$
5	5	5	3	4	(2) $\sqrt{\frac{1}{4}\sqrt{3}}$ , (2) $\sqrt{\frac{1}{4}\sqrt{30}}$
6	4	4	4	4	(2) $\sqrt{\frac{1}{4}\sqrt{3}}$ , (2) $\sqrt{\frac{1}{4}\sqrt{30}}$
6	5	4	3	4	(2) $\sqrt{\frac{1}{8}\sqrt{918-18\sqrt{1801}}}$ , (2) $\sqrt{\frac{1}{8}\sqrt{918+18\sqrt{1801}}}$
6	6	3	3	4	(2) $\sqrt{\frac{1}{4}\sqrt{183-3\sqrt{2641}}}$ , (2) $\sqrt{\frac{1}{4}\sqrt{183+3\sqrt{2641}}}$
6	6	5	3	4	(2) $\sqrt{\frac{1}{8}\sqrt{1602-18\sqrt{5281}}}$ , (2) $\sqrt{\frac{1}{8}\sqrt{1602+18\sqrt{5281}}}$
7	6	4	3	4	(2) $\sqrt{\frac{3}{4}\sqrt{6}}$ , (2) $\sqrt{\frac{3}{4}\sqrt{66}}$
7	7	7	3	4	(2) $\sqrt{\frac{15}{8}\sqrt{3}}$ , (2) $\sqrt{\frac{15}{8}\sqrt{715}}$

TABLE I. The Eigenvalues of the Volume for some 4-valent vertices

$P_0$	$P_1$	$P_2$	$P_3$	$P_4$	Dim.	$\lambda_{\beta_i} = \lambda_{\beta_i}(P_0, \dots, P_4)$
2	1	1	1	1	3	(3) $\sqrt{\frac{3\sqrt{2}+\sqrt{3}}{12}}$
2	2	2	1	1	4	(2) $\sqrt{\frac{29\sqrt{2}+12\sqrt{3}+16\sqrt{5}}{96}}$ , (1) $\sqrt{\frac{5\sqrt{2}+4\sqrt{5}}{16}}$ , (1) $\sqrt{\frac{5\sqrt{2}+4\sqrt{5}}{24}}$
2	2	2	2	2	6	(6) $\sqrt{\frac{5}{3}\sqrt{3}}$
3	2	1	1	1	3	(2) $\sqrt{\frac{21\sqrt{2}+6\sqrt{3}+18\sqrt{5}+14\sqrt{15}}{192}}$ , (1) $\sqrt{\frac{15\sqrt{2}+18\sqrt{5}+4\sqrt{15}}{96}}$
4	2	2	1	1	3	(1) $\sqrt{\frac{40+10\sqrt{2}+4\sqrt{5}+5\sqrt{6}}{80}}$ , (1) $\sqrt{\frac{60+15\sqrt{2}+20\sqrt{3}+12\sqrt{5}+10\sqrt{6}}{80}}$ , (1) $\sqrt{\frac{20+\sqrt{2}+4\sqrt{3}+4\sqrt{5}}{80}}$

TABLE II. The Eigenvalues of the Volume for some 5-valent vertices.

- 
- [1] R. Penrose, in *Magic Without Magic: John Archibald Wheeler*, edited by J. R. Klauder (W. H. Freeman and Company, San Francisco, 1972).
  - [2] C. Rovelli and L. Smolin, Phys. Rev. Lett. **61**, 1155 (1988).
  - [3] C. Rovelli and L. Smolin, Nucl. Phys. **B331**, 80 (1990).
  - [4] C. Isham, *Structural Issues in Quantum Gravity*, to appear in the proceedings of the GR14 (Florence 1995).
  - [5] *Diffeomorphism invariant quantum field theory and quantum geometry*. Special Issue of Journal of Mathematical Physics, J. Math. Phys. **36**, (1995).
  - [6] J. Baez, *Knots and Quantum Gravity* (Oxford University Press, Oxford, 1994).
  - [7] J. Ehlers and H. Friedrich, *Canonical Gravity: from Classical to Quantum* (Springer-Verlag, Berlin, 1994).
  - [8] C. Rovelli, Class. and Quantum Grav **8**, 1613 (1991).
  - [9] A. Ashtekar, in *Gravitation and Quantization, Les Houches, Session LVII, 1992*, edited by B. Julia and J. Zinn-Justin (Elsevier Science, 1995).
  - [10] C. Rovelli and L. Smolin, Phys. Rev. **D53**, 5743 (1995).
  - [11] J. C. Baez, *Spin Network States in Gauge Theories*, Advances in Mathematics, to appear (1999); *Spin Networks in Nonperturbative Quantum Gravity*, gr-qc/9504036.
  - [12] T. Foxon, Class. and Quant. Grav **12**, 951 (1995).
  - [13] A. Ashtekar, C. Rovelli, and L. Smolin, Phys. Rev. Lett. **69**, 237 (1992).
  - [14] C. Rovelli and L. Smolin, Nucl. Phys. **B442**, 593 (1995).
  - [15] R. Loll, Phys. Rev. Lett. **75**, 3048 (1995).
  - [16] C. Rovelli, Nucl. Phys. **B405**, 797 (1993).
  - [17] A. Ashtekar and C. Isham, Class. and Quantum Grav. **9**, 1433 (1992).
  - [18] A. Ashtekar, D. Lewandowsky, Jerzy Marolf, J. Mourao, and T. Thiemann, J. Math. Phys. **36**, 6456 (1995).
  - [19] C. Rovelli and L. Smolin, Phys. Rev. Lett. **72**, 446 (1994).
  - [20] C. Rovelli, J. Math. Phys. **36**, 6529 (1995).
  - [21] C. Rovelli and H. Morales-Tecotl, Phys. Rev. Lett. **72**, 3642 (1995); Nucl. Phys. **B451**, 325 (1995).
  - [22] K. Krasnov, *Quantum Loop Representation for Fermions coupled to Einstein-Maxwell field* gr-qc/9506029 (1995).
  - [23] R. Penrose, in *Combinatorial Mathematics and its Application*, edited by D. Welsh (Academic Press, New York, 1971).
  - [24] L. H. Kauffman and S. L. Lins, *Temperley-Lieb Recoupling Theory and Invariant of 3-Manifolds* (Princeton University Press, Princeton, 1994).
  - [25] M. Reisenberger, *Spin-network states and operators*, in preparation (1996).
  - [26] L. Smolin and S. Major, *Quantum deformation of quantum gravity* CGPG-95/12-3 (1995), gr-qc/9512020. L. Smolin, S. Major and R. Borissov, *The geometry of quantum spin networks*, CGPG-95/12-4 (1995), gr-qc/9512043.
  - [27] R. Borissov, *Eigenvalue spectrum of the Volume Operator in Quantum Gravity*, in preparation (1996).
  - [28] R. Loll, *Spectrum of the Volume Operator in Quantum Gravity* gr-qc/9511030.
  - [29] A. Ashtekar, Phys. Rev. Lett. **57**, 2244 (1986); Phys. Rev. **D36**, 1587 (1987). For an introduction to the Ashtekar formalism, see Ref. [8], or: A. Ashtekar, *Nonperturbative Canonical Gravity* (World Scientific, Singapore, 1991).
  - [30] R. Penrose, in *Quantum Theory and Beyond*, edited by T. Bastin (Cambridge University Press, Cambridge, 1971).
  - [31] C. Rovelli, E. T. Newman, and J. Lewandowski, J. Math. Phys. **34**, 4646 (1993).
  - [32] R. Gambini and A. Trias, Nucl. Phys. **B278**, 436 (1986); Phys. Rev. **D23**, 553 (1981).
  - [33] L. H. Kauffman, in *Knots, Topology and Quantum Field Theories*, edited by L. Lusanna (World Scientific, Singapore, 1991).
  - [34] M. Behzad and G. Chartrand, *Introduction to the Theory of Graphs* (Allyn and Bacon, Boston, 1971).
  - [35] K. Reidemeister, *Knotentheorie* (Julius Springer, Berlin, 1932).
  - [36] B. Brügmann, R. Gambini, and J. Pullin, Phys. Rev. Lett **68**, 431 (1992). B. Brügmann, R. Gambini, and J. Pullin, Nucl. Phys **B385**, 587 (1992). B. Brügmann, R. Gambini, and J. Pullin, Gen. Rel. Grav. **25**, 1 (1993). B. Brügmann, in *Canonical Gravity: From Classical to Quantum*, edited by J. Ehlers and H. Friedrich (Springer-Verlag, Berlin, 1993). J. Pullin, in *Proceedings of the Vth Mexican School of Particles and Fields*, edited by J. Lucio (World Scientific, Singapore, 1993).
  - [37] C. Rovelli, Phys. Rev. **D47**, 1703 (1993).
  - [38] L. Smolin, in *Brill Festschrift Proceedings*, edited by B. Hu and T. Jacobson (Cambridge University Press, Cambridge, 1993); in *Quantum Gravity and Cosmology* (World Scientific, Singapore, 1993).
  - [39] D. M. Brink and G. R. Satchler, *Angular Momentum* (Clarendon Press, Oxford, 1968).
  - [40] A. Ashtekar, J. Lewandowski, *Representation theory of analytic holonomy  $C^*$  algebras*, in [6].
  - [41] C. Rovelli, Class. and Quantum Grav. **8**, 297 (1991); Class. and Quantum Grav. **8**, 317 (1991).
  - [42] J. Iwasaki and C. Rovelli: Int. J. of Mod. Phys. **D1**, 533 (1993); Class. and Quantum Grav. **11**, 1653 (1994).

- [43] T. Thiemann, *Reality conditions inducing transforms for quantum gauge and quantum gravity*, gr-qc/951105. A. Ashtekar *A Generalized Wick Transform for Gravity*, gr-qc/9511083.
- [44] S. Hawking, *Comm. Math. Phys.*, **43**, 199 (1975).
- [45] L. H. Kauffman, *Trans. Amer. Math. Soc.* **318**, 417 (1990).
- [46] Moussoris, in *Advances in Twistor Theory, Research Notes in Mathematics*, edited by Huston and Ward (Pitman, 1979), pp. 308–312.
- [47] L. H. Kauffman, *Inter. Jour. of Modern Physics A*, **5**, 93 (1990).
- [48] I. Levinson, *Liet. TSR Mokslu Acad. Darbai B Ser.* **2**, 17 (1956).
- [49] A. P. Yutsin, J. B. Levinson, and V. V. Vanagas, *Mathematical Apparatus of the Theory of angular momentum* (Israel program for Scientific Translation, Jerusalem, 1962).